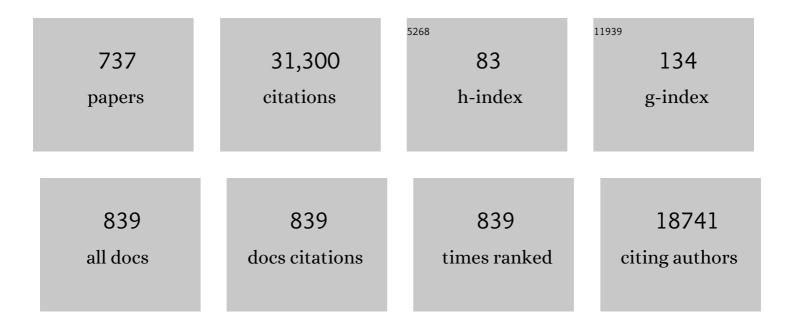
## Silvio Aime

List of Publications by Year in descending order

Source: https://exaly.com/author-pdf/4968472/publications.pdf Version: 2024-02-01



#	Article	IF	CITATIONS
1	Theranostic Nanomedicine. Accounts of Chemical Research, 2011, 44, 1029-1038.	15.6	765
2	Challenges for Molecular Magnetic Resonance Imaging. Chemical Reviews, 2010, 110, 3019-3042.	47.7	728
3	Lanthanide(III) chelates for NMR biomedical applications. Chemical Society Reviews, 1998, 27, 19-29.	38.1	698
4	Biodistribution of gadoliniumâ€based contrast agents, including gadolinium deposition. Journal of Magnetic Resonance Imaging, 2009, 30, 1259-1267.	3.4	444
5	Paramagnetic Lanthanide(III) complexes as pH-sensitive chemical exchange saturation transfer (CEST) contrast agents for MRI applications. Magnetic Resonance in Medicine, 2002, 47, 639-648.	3.0	365
6	Insights into the use of paramagnetic Gd(III) complexes in MR-molecular imaging investigations. Journal of Magnetic Resonance Imaging, 2002, 16, 394-406.	3.4	340
7	Conformational and Coordination Equilibria on DOTA Complexes of Lanthanide Metal Ions in Aqueous Solution Studied by 1H-NMR Spectroscopy. Inorganic Chemistry, 1997, 36, 2059-2068.	4.0	333
8	Pushing the Sensitivity Envelope of Lanthanide-Based Magnetic Resonance Imaging (MRI) Contrast Agents for Molecular Imaging Applications. Accounts of Chemical Research, 2009, 42, 822-831.	15.6	327
9	NMR study of solution structures and dynamics of lanthanide(III) complexes of DOTA. Inorganic Chemistry, 1992, 31, 4291-4299.	4.0	323
10	Gd(III)-BASED CONTRAST AGENTS FOR MRI. Advances in Inorganic Chemistry, 2005, 57, 173-237.	1.0	307
11	The Selectivity of Reversible Oxy-Anion Binding in Aqueous Solution at a Chiral Europium and Terbium Center:Â Signaling of Carbonate Chelation by Changes in the Form and Circular Polarization of Luminescence Emission. Journal of the American Chemical Society, 2000, 122, 9674-9684.	13.7	292
12	High sensitivity lanthanide(III) based probes for MR-medical imaging. Coordination Chemistry Reviews, 2006, 250, 1562-1579.	18.8	284
13	pH-Dependent Modulation of Relaxivity and Luminescence in Macrocyclic Gadolinium and Europium Complexes Based on Reversible Intramolecular Sulfonamide Ligation. Journal of the American Chemical Society, 2001, 123, 7601-7609.	13.7	269
14	NMR, Relaxometric, and Structural Studies of the Hydration and Exchange Dynamics of Cationic Lanthanide Complexes of Macrocyclic Tetraamide Ligands. Journal of the American Chemical Society, 1999, 121, 5762-5771.	13.7	267
15	Compartmentalization of a Gadolinium Complex in the Apoferritin Cavity: A Route To Obtain High Relaxivity Contrast Agents for Magnetic Resonance Imaging. Angewandte Chemie - International Edition, 2002, 41, 1017-1019.	13.8	265
16	Structural, Luminescence, and NMR Studies of the Reversible Binding of Acetate, Lactate, Citrate, and Selected Amino Acids to Chiral Diaqua Ytterbium, Gadolinium, and Europium Complexes. Journal of the American Chemical Society, 2002, 124, 12697-12705.	13.7	246
17	[Gd-AAZTA]-:Â A New Structural Entry for an Improved Generation of MRI Contrast Agents. Inorganic Chemistry, 2004, 43, 7588-7590.	4.0	217
18	ParaHydrogen Induced Polarization of 13C carboxylate resonance in acetate and pyruvate. Nature Communications, 2015, 6, 5858.	12.8	206

#	Article	IF	CITATIONS
19	Prototropic and Water-Exchange Processes in Aqueous Solutions of Gd(III) Chelates. Accounts of Chemical Research, 1999, 32, 941-949.	15.6	198
20	Novel pH-Reporter MRI Contrast Agents. Angewandte Chemie - International Edition, 2002, 41, 4334-4336.	13.8	198
21	Correlation of Water Exchange Rate with Isomeric Composition in Diastereoisomeric Gadolinium Complexes of Tetra(carboxyethyl)dota and Related Macrocyclic Ligands. Journal of the American Chemical Society, 2000, 122, 9781-9792.	13.7	189
22	Probing Protein Conformation in Cells by EPR Distance Measurements using Gd <sup>3+</sup> Spin Labeling. Journal of the American Chemical Society, 2014, 136, 13458-13465.	13.7	187
23	Highly Sensitive MRI Chemical Exchange Saturation Transfer Agents Using Liposomes. Angewandte Chemie - International Edition, 2005, 44, 5513-5515.	13.8	185
24	A Paramagnetic MRI-CEST Agent Responsive to Lactate Concentration. Journal of the American Chemical Society, 2002, 124, 9364-9365.	13.7	182
25	Novel Contrast Agents for Magnetic Resonance Imaging. Synthesis and Characterization of the Ligand BOPTA and Its Ln(III) Complexes (Ln = Gd, La, Lu). X-ray Structure of Disodium (TPS-9-145337286-C-S)-[4-Carboxy-5,8,11-tris(carboxymethyl)-1-phenyl-2-oxa- 5,8,11-triazatridecan-13-oato(5-)]gadolinate(2-) in a Mixture with Its Enantiomer. Inorganic Chemistry,	4.0	180
26	1995, ort. Goordated Iopamidol as a responsive MRIâ€chemical exchange saturation transfer contrast agent for pH mapping of kidneys: In vivo studies in mice at 7 T. Magnetic Resonance in Medicine, 2011, 65, 202-211.	3.0	178
27	Tunable Imaging of Cells Labeled with MRI-PARACEST Agents. Angewandte Chemie - International Edition, 2005, 44, 1813-1815.	13.8	170
28	Gd(III) complexes as contrast agents for magnetic resonance imaging: a proton relaxation enhancement study of the interaction with human serum albumin. Journal of Biological Inorganic Chemistry, 1996, 1, 312-319.	2.6	167
29	High Relaxivity Gadolinium Hydroxypyridonateâ^'Viral Capsid Conjugates:  Nanosized MRI Contrast Agents <sup>1</sup> . Journal of the American Chemical Society, 2008, 130, 2546-2552.	13.7	165
30	First17O NMR Observation of Coordinated Water on Both Isomers of [Eu(DOTAM)(H2O)]3+:Â A Direct Access to Water Exchange and its Role in the Isomerization1. Journal of the American Chemical Society, 2000, 122, 1506-1512.	13.7	163
31	Effect of the intracellular localization of a Gdâ€based imaging probe on the relaxation enhancement of water protons. Magnetic Resonance in Medicine, 2006, 55, 491-497.	3.0	158
32	A General MRI-CEST Ratiometric Approach for pH Imaging: Demonstration of <i>in Vivo</i> pH Mapping with lobitridol. Journal of the American Chemical Society, 2014, 136, 14333-14336.	13.7	155
33	Solution and Solid-State Characterization of Highly Rigid, Eight-Coordinate Lanthanide(III) Complexes of a Macrocyclic Tetrabenzylphosphinate. Inorganic Chemistry, 1994, 33, 4696-4706.	4.0	152
34	Improved route for the visualization of stem cells labeled with a Gdâ€ <b>/</b> Euâ€Chelate as dual (MRI and) Tj ETQqO C	) 0 rgBT /O	verlock 10 Tf
35	Ap(O2)-Responsive MRI Contrast Agent Based on the Redox Switch of Manganese(II /III) - Porphyrin Complexes. Angewandte Chemie - International Edition, 2000, 39, 747-750.	13.8	150

Crystal structure and solution dynamics of the lutetium(III) chelate of DOTA. Inorganica Chimica Acta, 2.4 141

#	Article	IF	CITATIONS
37	Ternary Gd(III)L-HSA adducts: evidence for the replacement of inner-sphere water molecules by coordinating groups of the protein. Implications for the design of contrast agents for MRI. Journal of Biological Inorganic Chemistry, 2000, 5, 488-497.	2.6	140
38	Structural Variations Across the Lanthanide Series of Macrocyclic DOTA Complexes:Â Insights into the Design of Contrast Agents for Magnetic Resonance Imaging. Inorganic Chemistry, 2003, 42, 148-157.	4.0	140
39	Copper-Responsive Magnetic Resonance Imaging Contrast Agents. Journal of the American Chemical Society, 2009, 131, 8527-8536.	13.7	139
40	Image guided therapy: The advent of theranostic agents. Journal of Controlled Release, 2012, 161, 328-337.	9.9	136
41	<i>In Vivo</i> Imaging of Tumor Metabolism and Acidosis by Combining PET and MRI-CEST pH Imaging. Cancer Research, 2016, 76, 6463-6470.	0.9	134
42	Direct NMR Spectroscopic Observation of a Lanthanideâ€Coordinated Water Molecule whose Exchange Rate Is Dependent on the Conformation of the Complexes. Angewandte Chemie - International Edition, 1998, 37, 2673-2675.	13.8	133
43	Magnetic Resonance Visualization of Tumor Angiogenesis by Targeting Neural Cell Adhesion Molecules with the Highly Sensitive Gadolinium-Loaded Apoferritin Probe. Cancer Research, 2006, 66, 9196-9201.	0.9	132
44	NMR relaxometric studies of Gd(III) complexes with heptadentate macrocyclic ligands. Magnetic Resonance in Chemistry, 1998, 36, S200-S208.	1.9	129
45	Effect of ibuprofen and warfarin on the allosteric properties of haem-human serum albumin. FEBS Journal, 2001, 268, 6214-6220.	0.2	123
46	Synthesis, characterization, and 1/T1 NMRD profiles of gadolinium(III) complexes of monoamide derivatives of DOTA-like ligands. X-ray structure of the 10-[2-[[2-hydroxy-1-(hydroxymethyl)ethyl]amino]-1-[(phenylmethoxy)methyl]-2-oxoethyl]-1,4,7,10-tetraazacyc acid-gadolinium(III) complex. Inorganic Chemistry, 1992, 31, 2422-2428.	lodođecan	e-1,4,7-triace1
47	Synthesis and NMR Studies of Three Pyridine-Containing Triaza Macrocyclic Triacetate Ligands and Their Complexes with Lanthanide Ions. Inorganic Chemistry, 1997, 36, 2992-3000.	4.0	119
48	The 13C hyperpolarized pyruvate generated by ParaHydrogen detects the response of the heart to altered metabolism in real time. Scientific Reports, 2018, 8, 8366.	3.3	119
49	Metal containing nanosized systems for MR-Molecular Imaging applications. Coordination Chemistry Reviews, 2008, 252, 2424-2443.	18.8	116
50	lopamidol: Exploring the potential use of a well-established x-ray contrast agent for MRI. Magnetic Resonance in Medicine, 2005, 53, 830-834.	3.0	115
51	Imaging the pH evolution of an acute kidney injury model by means of iopamidol, a MRI-CEST pH-responsive contrast agent. Magnetic Resonance in Medicine, 2013, 70, 859-864.	3.0	114
52	Encoding the frequency dependence in MRI contrast media: the emerging class of CEST agents. Contrast Media and Molecular Imaging, 2010, 5, 78-98.	0.8	113
53	Ln(III)-DOTAMGly Complexes: A Versatile Series to Assess the Determinants of the Efficacy of Paramagnetic Chemical Exchange Saturation Transfer Agents for Magnetic Resonance Imaging Applications. Investigative Radiology, 2004, 39, 235-243.	6.2	112
54	PrototropicvsWhole Water Exchange Contributions to the Solvent Relaxation Enhancement in the Aqueous Solution of a Cationic Gd3+Macrocyclic Complex. Journal of the American Chemical Society, 1997, 119, 4767-4768.	13.7	108

#	Article	IF	CITATIONS
55	PAMAM Dendrimeric Conjugates with a Gdâ^'DOTA Phosphinate Derivative and Their Adducts with Polyaminoacids:Â The Interplay of Global Motion, Internal Rotation, and Fast Water Exchange. Bioconjugate Chemistry, 2006, 17, 975-987.	3.6	108
56	Yb <sup>III</sup> â€HPDO3A: A Dual pH―and Temperatureâ€Responsive CEST Agent. Angewandte Chemie - International Edition, 2011, 50, 1798-1800.	13.8	103
57	Development and validation of a smoothingâ€splinesâ€based correction method for improving the analysis of CESTâ€MR images. Contrast Media and Molecular Imaging, 2008, 3, 136-149.	0.8	102
58	In VitroandIn VivoStudy of Solid Lipid Nanoparticles Loaded with Superparamagnetic Iron Oxide. Journal of Drug Targeting, 2003, 11, 19-24.	4.4	100
59	Contrast agents for magnetic resonance angiographic applications: 1H and 17O NMR relaxometric investigations on two gadolinium(III) DTPA-like chelates endowed with high binding affinity to human serum albumin. Journal of Biological Inorganic Chemistry, 1999, 4, 766-774.	2.6	99
60	Highâ€Relaxivity Magnetic Resonance Imaging (MRI) Contrast Agent Based on Supramolecular Assembly between a Gadolinium Chelate, a Modified Dextran, and Polyâ€Î²â€Cyclodextrin. Chemistry - A European Journal, 2008, 14, 4551-4561.	3.3	99
61	Relaxometric evaluation of novel manganese(II) complexes for application as contrast agents in magnetic resonance imaging. Journal of Biological Inorganic Chemistry, 2002, 7, 58-67.	2.6	98
62	In vivo maps of extracellular pH in murine melanoma by CEST–MRI. Magnetic Resonance in Medicine, 2014, 71, 326-332.	3.0	98
63	Highly Soluble Tris-hydroxypyridonate Gd(III) Complexes with Increased Hydration Number, Fast Water Exchange, Slow Electronic Relaxation, and High Relaxivity1. Journal of the American Chemical Society, 2007, 129, 1870-1871.	13.7	97
64	Targeting Cells with MR Imaging Probes Based on Paramagnetic Gd(III) Chelates. Current Pharmaceutical Biotechnology, 2004, 5, 509-518.	1.6	97
65	NMR Evidence of a Long Exchange Lifetime for the Coordinated Water in Ln(III)-Bis(methyl amide)-DTPA Complexes (Ln = Gd, Dy). Inorganic Chemistry, 1994, 33, 4707-4711.	4.0	95
66	Syntheses and Relaxation Properties of Mixed Gadolinium Hydroxypyridinonate MRI Contrast Agents. Inorganic Chemistry, 2000, 39, 5747-5756.	4.0	95
67	Relaxometric and Modelling Studies of the Binding of a Lipophilic Gd-AAZTA Complex to Fatted and Defatted Human Serum Albumin. Chemistry - A European Journal, 2007, 13, 5785-5797.	3.3	93
68	A R2/R1Ratiometric Procedure for a Concentration-Independent, pH-Responsive, Gd(III)-Based MRI Agent. Journal of the American Chemical Society, 2006, 128, 11326-11327.	13.7	92
69	Gadolinium Retention in the Rat Brain: Assessment of the Amounts of Insoluble Gadolinium-containing Species and Intact Gadolinium Complexes after Repeated Administration of Gadolinium-based Contrast Agents. Radiology, 2017, 285, 839-849.	7.3	92
70	Dual-modality gene reporter for in vivo imaging. Proceedings of the National Academy of Sciences of the United States of America, 2014, 111, 415-420.	7.1	91
71	Proteomics as a tool to improve investigation of substantial equivalence in genetically modified organisms: The case of a virusâ€resistant tomato. Proteomics, 2004, 4, 193-200.	2.2	90
72	Equilibrium and Kinetic Properties of the Lanthanoids(III) and Various Divalent Metal Complexes of the Heptadentate Ligand AAZTA. Chemistry - A European Journal, 2009, 15, 1696-1705.	3.3	90

#	Article	IF	CITATIONS
73	Combined Delivery and Magnetic Resonance Imaging of Neural Cell Adhesion Molecule–Targeted Doxorubicin-Containing Liposomes in Experimentally Induced Kaposi's Sarcoma. Cancer Research, 2010, 70, 2180-2190.	0.9	90
74	Cellular labeling with Gd(III) chelates: only high thermodynamic stabilities prevent the cells acting as †sponges' of Gd3+ ions. Contrast Media and Molecular Imaging, 2006, 1, 23-29.	0.8	89
75	NMR relaxometric investigations of solid lipid nanoparticles (SLN) containing gadolinium(III) complexes. European Journal of Pharmaceutics and Biopharmaceutics, 1998, 45, 157-163.	4.3	88
76	A Novel Compound in the Lanthanide(III) DOTA Series. X-ray Crystal and Molecular Structure of the Complex Na[La(DOTA)La(HDOTA)]·10H2O. Inorganic Chemistry, 1997, 36, 4287-4289.	4.0	87
77	Optimization of the Relaxivity of MRI Contrast Agents:  Effect of Poly(ethylene glycol) Chains on the Water-Exchange Rates of GdIII Complexes. Journal of the American Chemical Society, 2001, 123, 10758-10759.	13.7	87
78	Ternary Complexes between Cationic GdIII Chelates and Anionic Metabolites in Aqueous Solution: An NMR Relaxometric Study. Chemistry - A European Journal, 2003, 9, 2102-2109.	3.3	87
79	From Spherical to Osmotically Shrunken Paramagnetic Liposomes: An Improved Generation of LIPOCEST MRI Agents with Highly Shifted Water Protons. Angewandte Chemie - International Edition, 2007, 46, 966-968.	13.8	87
80	Dissociation Kinetics of Openâ€Chain and Macrocyclic Gadolinium(III)â€Aminopolycarboxylate Complexes Related to Magnetic Resonance Imaging: Catalytic Effect of Endogenous Ligands. Chemistry - A European Journal, 2012, 18, 16426-16435.	3.3	87
81	[GdPCP2A(H2O)2]-: A Paramagnetic Contrast Agent Designed for Improved Applications in Magnetic Resonance Imaging. Journal of Medicinal Chemistry, 2000, 43, 4017-4024.	6.4	86
82	Properties, Solution State Behavior, and Crystal Structures of Chelates of DOTMA. Inorganic Chemistry, 2011, 50, 7955-7965.	4.0	86
83	Magnetic resonance imaging of gadolinium-labeled pancreatic islets for experimental transplantation. NMR in Biomedicine, 2007, 20, 40-48.	2.8	85
84	Synthesis of a bifunctional monophosphinic acid DOTA analogue ligand and its lanthanide(iii) complexes. A gadolinium(iii) complex endowed with an optimal water exchange rate for MRI applications. Organic and Biomolecular Chemistry, 2005, 3, 112-117.	2.8	84
85	Glycoconjugates of gadolinium complexes for MRI applications. Chemical Communications, 2006, , 1064.	4.1	84
86	A new ytterbium chelate as contrast agent in chemical shift imaging and temperature sensitive probe for MR spectroscopy. Magnetic Resonance in Medicine, 1996, 35, 648-651.	3.0	83
87	A macromolecular Gd(III) complex as pH-responsive relaxometric probe for MRI applications. Chemical Communications, 1999, , 1577-1578.	4.1	83
88	A Tris-hydroxymethyl-Substituted Derivative of Gd-TREN-Me-3,2-HOPO:  An MRI Relaxation Agent with Improved Efficiency. Journal of the American Chemical Society, 2000, 122, 11228-11229.	13.7	83
89	Gd-Loaded Liposomes asT1, Susceptibility, and CEST Agents, All in One. Journal of the American Chemical Society, 2007, 129, 2430-2431.	13.7	83
90	Nuclear magnetic resonance, luminescence and structural studies of lanthanide complexes with octadentate macrocyclic ligands bearing benzylphosphinate groups. Journal of the Chemical Society Dalton Transactions, 1997, , 3623-3636.	1.1	82

#	Article	IF	CITATIONS
91	Substituent Effects on Gd(III)-Based MRI Contrast Agents:  Optimizing the Stability and Selectivity of the Complex and the Number of Coordinated Water Molecules1. Inorganic Chemistry, 2006, 45, 8355-8364.	4.0	82
92	A Highly Stable Gadolinium Complex with a Fast, Associative Mechanism of Water Exchange. Journal of the American Chemical Society, 2003, 125, 14274-14275.	13.7	81
93	MRI Visualization of Melanoma Cells by Targeting Overexpressed Sialic Acid with a Gd <sup>III</sup> â€dotaâ€enâ€pba Imaging Reporter. Angewandte Chemie - International Edition, 2013, 52, 1161-1164.	13.8	81
94	Review and consensus recommendations on clinical <scp>APT</scp> â€weighted imaging approaches at <scp>3T</scp> : Application to brain tumors. Magnetic Resonance in Medicine, 2022, 88, 546-574.	3.0	79
95	Relaxometric, Structural, and Dynamic NMR Studies of DOTA-like Ln(III) Complexes (Ln = La, Gd, Ho, Yb) Containing ap-Nitrophenyl Substituent. Inorganic Chemistry, 1996, 35, 2726-2736.	4.0	77
96	Towards MRI contrast agents of improved efficacy. NMR relaxometric investigations of the binding interaction to HSA of a novel heptadentate macrocyclic triphosphonate Gd(III)-complex. Journal of Biological Inorganic Chemistry, 1997, 2, 470-479.	2.6	77
97	Platinum(II)–Gadolinium(III) Complexes as Potential Singleâ€Molecular Theranostic Agents for Cancer Treatment. Angewandte Chemie - International Edition, 2014, 53, 13225-13228.	13.8	77
98	Paramagnetic Liposomes as Innovative Contrast Agents for Magnetic Resonance (MR) Molecular Imaging Applications. Chemistry and Biodiversity, 2008, 5, 1901-1912.	2.1	76
99	Designing Novel Contrast Agents for Magnetic Resonance Imaging. Synthesis and Relaxometric Characterization of three Gadolinium(III) Complexes Based on Functionalized Pyridine-Containing Macrocyclic Ligands. Helvetica Chimica Acta, 2003, 86, 615-632.	1.6	75
100	A Multinuclear NMR Study on the Structure and Dynamics of Lanthanide(III) Complexes of the Poly(amino carboxylate) EGTA4-in Aqueous Solution. Inorganic Chemistry, 1997, 36, 5104-5112.	4.0	74
101	Supramolecular Adducts between Poly-L-arginine and[TmlIIdotp]: A Route to Sensitivity-Enhanced Magnetic Resonance Imaging–Chemical Exchange Saturation Transfer Agents. Angewandte Chemie - International Edition, 2003, 42, 4527-4529.	13.8	74
102	Para-hydrogen enrichment and hyperpolarization. Concepts in Magnetic Resonance Part A: Bridging Education and Research, 2006, 28A, 321-330.	0.5	73
103	Functionalized Nanocontainers as Dual Magnetic and Optical Probes for Molecular Imaging Applications. Chemistry of Materials, 2008, 20, 5888-5893.	6.7	73
104	Current concepts on hyperpolarized molecules in MRI. Current Opinion in Chemical Biology, 2010, 14, 90-96.	6.1	73
105	Gd(DOTP)5- outer-sphere relaxation enhancement promoted by nitrogen bases. Magnetic Resonance in Medicine, 1993, 30, 583-591.	3.0	71
106	Dependence of the relaxivity and luminescence of gadolinium and europium amino-acid complexes on hydrogencarbonate and pH. Chemical Communications, 1999, , 1047-1048.	4.1	71
107	Determination of water permeability of paramagnetic liposomes of interest in MRI field. Journal of Inorganic Biochemistry, 2008, 102, 1112-1119.	3.5	70
108	Studies to enhance the hyperpolarization level in PHIP-SAH-produced C13-pyruvate. Journal of Magnetic Resonance, 2018, 289, 12-17.	2.1	70

#	Article	IF	CITATIONS
109	Extent of hydration of octadentate lanthanide complexes incorporating phosphinate donors: solution relaxometry and luminescence studies. Journal of the Chemical Society Dalton Transactions, 1996, , 17.	1.1	69
110	Non-covalent Conjugates between Cationic Polyamino Acids and GdIII Chelates: A Route for Seeking Accumulation of MRI-Contrast Agents at Tumor Targeting Sites. Chemistry - A European Journal, 2000, 6, 2609-2617.	3.3	69
111	High-Relaxivity Contrast Agents for Magnetic Resonance Imaging Based on Multisite Interactions between al̂2-Cyclodextrin Oligomer and Suitably Functionalized GdIII Chelates. Chemistry - A European Journal, 2001, 7, 5261-5269.	3.3	69
112	Controlling the variation of axial water exchange rates in macrocyclic lanthanide(iii) complexesElectronic supplementary information (ESI) available: experimental section. See http://www.rsc.org/suppdata/cc/b2/b202862j/. Chemical Communications, 2002, , 1120-1121.	4.1	69
113	In Vitro and in Vivo Magnetic Resonance Detection of Tumor Cells by Targeting Glutamine Transporters with Gd-Based Probes. Journal of Medicinal Chemistry, 2006, 49, 4926-4936.	6.4	69
114	Targeting ferritin receptors for the selective delivery of imaging and therapeutic agents to breast cancer cells. Nanoscale, 2015, 7, 6527-6533.	5.6	67
115	Novel Paramagnetic Macromolecular Complexes Derived from the Linkage of a Macrocyclic Gd(III) Complex to Polyamino Acids through a Squaric Acid Moiety. Bioconjugate Chemistry, 1999, 10, 192-199.	3.6	66
116	Effects of Magnetic Field Cycle on the Polarization Transfer from Parahydrogen to Heteronuclei through Long-Range J-Couplings. Journal of Physical Chemistry B, 2015, 119, 10035-10041.	2.6	66
117	{DOTA-bis(amide)}lanthanide Complexes: NMR Evidence for Differences in Water-Molecule Exchange Rates for Coordination Isomers. Chemistry - A European Journal, 2001, 7, 288-296.	3.3	65
118	Synthesis, Potentiometric, Kinetic, and NMR Studies of 1,4,7,10-Tetraazacyclododecane-1,7-bis(acetic) Tj ETQq Lanthanide(III) Ions. Inorganic Chemistry, 2008, 47, 3851-3862.	0 0 0 rgBT 4.0	/Overlock 10 65
119	In vivo MRI multicontrast kinetic analysis of the uptake and intracellular trafficking of paramagnetically labeled liposomes. Journal of Controlled Release, 2010, 144, 271-279.	9.9	64
120	Non-ionic Ln(III) chelates as MRI contrast agents: Synthesis, characterisation and 1H NMR relaxometric investigations of bis(benzylamide)diethylenetriaminepentaacetic acid Lu(III) and Gd(III) complexes. Inorganica Chimica Acta, 1997, 254, 63-70.	2.4	63
121	A responsive MRI contrast agent to monitor functional cell status. NeuroImage, 2006, 32, 1142-1149.	4.2	63
122	Fast field-cycling magnetic resonance imaging. Comptes Rendus Physique, 2010, 11, 136-148.	0.9	63
123	Synthesis and NMRD studies of gadolinium(3+) complexes of macrocyclic polyamino polycarboxylic ligands bearing .betabenzyloxyalphapropionic residues. Inorganic Chemistry, 1992, 31, 1100-1103.	4.0	62
124	Towards Targeted MRI: New MRI Contrast Agents for Sialic Acid Detection. Chemistry - A European Journal, 2004, 10, 5205-5217.	3.3	62
125	High-Relaxivity Gadolinium-Modified High-Density Lipoproteins as Magnetic Resonance Imaging Contrast Agents. Journal of Physical Chemistry B, 2009, 113, 6283-6289.	2.6	62
126	Nanoparticleâ€based chemical exchange saturation transfer (CEST) agents. NMR in Biomedicine, 2013, 26, 839-849.	2.8	62

#	Article	IF	CITATIONS
127	Preparation and in vitro characterization of chitosan nanobubbles as theranostic agents. Colloids and Surfaces B: Biointerfaces, 2015, 129, 39-46.	5.0	62
128	Stereochemically nonrigid carbonyl complexes of group VIII B metal clusters. Inorganica Chimica Acta, 1975, 15, 53-56.	2.4	61
129	Longitudinal Nuclear Relaxation in an A2Spin System Initially Polarized through Para-Hydrogen. Journal of the American Chemical Society, 1998, 120, 6770-6773.	13.7	61
130	Curcumin/Gd Loaded Apoferritin: A Novel "Theranostic―Agent To Prevent Hepatocellular Damage in Toxic Induced Acute Hepatitis. Molecular Pharmaceutics, 2013, 10, 2079-2085.	4.6	61
131	Butadienic derivatives and metal carbonyls II. Some rearrangements of butadienic ligands in reactions with dodecacarbonyltriruthenium. Inorganica Chimica Acta, 1974, 8, 71-75.	2.4	60
132	Poly-β-cyclodextrin based platform for pH mapping via a ratiometric 19F/1H MRI method. Chemical Communications, 2009, , 6044.	4.1	60
133	1H and 13C NMR studies of acetylenic complexes of Co2(CO)8. Inorganica Chimica Acta, 1977, 22, 135-139.	2.4	59
134	Magnetic Resonance Imaging Detection of Tumor Cells by Targeting Low-Density Lipoprotein Receptors with Gd-Loaded Low-Density Lipoprotein Particles. Neoplasia, 2007, 9, 1046-1056.	5.3	59
135	Inclusion complexes between β-cyclodextrin and β-benzyloxy-α-propionic derivatives of paramagnetic DOTA- and DPTA-Gd(III) complexes. Magnetic Resonance in Chemistry, 1991, 29, 923-927.	1.9	58
136	1,2-Hydroxypyridonates as Contrast Agents for Magnetic Resonance Imaging:  TREN-1,2-HOPO. Inorganic Chemistry, 2007, 46, 9182-9191.	4.0	58
137	New Hyperpolarized Contrast Agents for 13C-MRI from Para-Hydrogenation of Oligooxyethylenic Alkynes. Journal of the American Chemical Society, 2008, 130, 15047-15053.	13.7	58
138	Improved paramagnetic liposomes for MRI visualization of pH triggered release. Journal of Controlled Release, 2011, 154, 196-202.	9.9	58
139	In vivo MRI visualization of different cell populations labeled with PARACEST agents. Magnetic Resonance in Medicine, 2013, 69, 1703-1711.	3.0	58
140	Dendrimeric Gd(iii) complex of a monophosphinated DOTA analogue: optimizing relaxivity by reducing internal motion. Chemical Communications, 2005, , 2390.	4.1	57
141	Paramagnetic selfâ€assembled nanoparticles as supramolecular MRI contrast agents. Contrast Media and Molecular Imaging, 2012, 7, 356-361.	0.8	57
142	Controlled mixing of lanthanide(iii) ions in coacervate core micelles. Chemical Communications, 2013, 49, 3736.	4.1	57
143	In vivo evaluation of tumour acidosis for assessing the early metabolic response and onset of resistance to dichloroacetate by using magnetic resonance pH imaging. International Journal of Oncology, 2017, 51, 498-506.	3.3	57
144	A generalized ratiometric chemical exchange saturation transfer (CEST) MRI approach for mapping renal pH using iopamidol. Magnetic Resonance in Medicine, 2018, 79, 1553-1558.	3.0	57

#	Article	IF	CITATIONS
145	The RNA-binding protein ESRP1 promotes human colorectal cancer progression. Oncotarget, 2017, 8, 10007-10024.	1.8	57
146	NMR conformational study of the lanthanide(III) complexes of DOTA in aqueous solution. Journal of Alloys and Compounds, 1995, 225, 303-307.	5.5	56
147	MRIâ€Guided Neutron Capture Therapy by Use of a Dual Gadolinium/Boron Agent Targeted at Tumour Cells through Upregulated Lowâ€Density Lipoprotein Transporters. Chemistry - A European Journal, 2011, 17, 8479-8486.	3.3	56
148	<sup>13</sup> Câ€MR Hyperpolarization of Lactate by Using ParaHydrogen and Metabolic Transformation in Vitro. Chemistry - A European Journal, 2017, 23, 1200-1204.	3.3	56
149	Gadolinium-Enhanced Magnetic Resonance Imaging, Renal Failure and Nephrogenic Systemic Fibrosis /Nephrogenic Fibrosing Dermopathy. Current Medicinal Chemistry, 2008, 15, 1229-1235.	2.4	55
150	Para-hydrogenated Glucose Derivatives as Potential <sup>13</sup> C-Hyperpolarized Probes for Magnetic Resonance Imaging. Journal of the American Chemical Society, 2010, 132, 7186-7193.	13.7	55
151	Use of Labile Precursors for the Generation of Hyperpolarized Molecules from Hydrogenation with Parahydrogen and Aqueousâ€Phase Extraction. Angewandte Chemie - International Edition, 2011, 50, 7350-7353.	13.8	55
152	Determination of metal–proton distances and electronic relaxation times in lanthanide complexes by nuclear magnetic resonance spectroscopy. Journal of the Chemical Society Dalton Transactions, 1992, , 225-228.	1.1	54
153	On the role of the counter-ion in defining water structure and dynamics: order, structure and dynamics in hydrophilic and hydrophobic gadolinium salt complexes. Dalton Transactions, 2006, , 5605.	3.3	54
154	Methods for an improved detection of the MRIâ€CEST effect. Contrast Media and Molecular Imaging, 2009, 4, 237-247.	0.8	54
155	Rapid hyperpolarization and purification of the metabolite fumarate in aqueous solution. Proceedings of the National Academy of Sciences of the United States of America, 2021, 118, .	7.1	54
156	L-Ferritin targets breast cancer stem cells and delivers therapeutic and imaging agents. Oncotarget, 2016, 7, 66713-66727.	1.8	54
157	Quantitative description of radiofrequency (RF) powerâ€based ratiometric chemical exchange saturation transfer (CEST) pH imaging. NMR in Biomedicine, 2015, 28, 555-565.	2.8	53
158	AAZTA: An Ideal Chelating Agent for the Development of <sup>44</sup> Sc PET Imaging Agents. Angewandte Chemie - International Edition, 2017, 56, 2118-2122.	13.8	53
159	EPR investigations of the iron domain in neuromelanin. Biochimica Et Biophysica Acta - Molecular Basis of Disease, 1997, 1361, 49-58.	3.8	52
160	The Structure of the Sugar Residue in Glycated Human Serum Albumin and Its Molecular Recognition by Phenylboronate. Chemistry - A European Journal, 2003, 9, 2193-2199.	3.3	52
161	Combined High Resolution NMR and <sup>1</sup> H and <sup>17</sup> O Relaxometric Study Sheds Light on the Solution Structure and Dynamics of the Lanthanide(III) Complexes of HPDO3A. Inorganic Chemistry, 2013, 52, 7130-7138.	4.0	52
162	Sonosensitive theranostic liposomes for preclinical in vivo MRI-guided visualization of doxorubicin release stimulated by pulsed low intensity non-focused ultrasound. Journal of Controlled Release, 2015, 202, 21-30.	9.9	52

#	Article	IF	CITATIONS
163	NMR Evidence for Interconversion between Two Enantiomeric Forms of Macrocyclic Schiff Base Lanthanide(III) Complexes Through Reversible Ring Contraction and Expansion. Inorganic Chemistry, 1995, 34, 5825-5831.	4.0	51
164	Quantification of the expression level of integrin receptor $\hat{1}\pm v\hat{1}^23$ in cell lines and MR imaging with antibody-coated iron oxide particles. Magnetic Resonance in Medicine, 2006, 56, 711-716.	3.0	51
165	A copper-activated magnetic resonance imaging contrast agent with improved turn-on relaxivity response and anion compatibility. Dalton Transactions, 2010, 39, 469-476.	3.3	51
166	β-Gal Gene Expression MRI Reporter in Melanoma Tumor Cells. Design, Synthesis, and <i>in Vitro</i> and <i>in Vivo</i> Testing of a Gd(III) Containing Probe Forming a High Relaxivity, Melanin-Like Structure upon β-Gal Enzymatic Activation. Bioconjugate Chemistry, 2011, 22, 2625-2635.	3.6	51
167	A theranostic approach based on the use of a dual boron/Gd agent to improve the efficacy of Boron Neutron Capture Therapy in the lung cancer treatment. Nanomedicine: Nanotechnology, Biology, and Medicine, 2015, 11, 741-750.	3.3	51
168	A Multinuclear NMR Relaxometry Study of Ternary Adducts Formed between Heptadentate GdIII Chelates andL-Lactate. Chemistry - A European Journal, 2005, 11, 5531-5537.	3.3	50
169	Osmotically Shrunken LIPOCEST Agents: An Innovative Class of Magnetic Resonance Imaging Contrast Media Based on Chemical Exchange Saturation Transfer. Chemistry - A European Journal, 2009, 15, 1440-1448.	3.3	50
170	Solution Structures, Stabilities, Kinetics, and Dynamics of DO3A and DO3A–Sulphonamide Complexes. Inorganic Chemistry, 2014, 53, 2858-2872.	4.0	50
171	Real-Time Nuclear Magnetic Resonance Detection of Fumarase Activity Using Parahydrogen-Hyperpolarized [1- <sup>13</sup> C]Fumarate. Journal of the American Chemical Society, 2019, 141, 20209-20214.	13.7	50
172	Characterisation of magnetic resonance imaging (MRI) contrast agents using NMR relaxometry. Molecular Physics, 2019, 117, 898-909.	1.7	50
173	Structural determinants of fluoride and formate binding to hemoglobin and myoglobin: crystallographic and 1H-NMR relaxometric study. Biophysical Journal, 1996, 70, 482-488.	0.5	49
174	Relaxometric and luminescence behaviour of triaquahexaazamacrocyclic complexes, the gadolinium complex displaying a high relaxivity with a pronounced pH dependence. New Journal of Chemistry, 1998, 22, 627-631.	2.8	49
175	Modulation of the water exchange rates in [Gd–DO3A] complex by formation of ternary complexes with carboxylate ligands. Chemical Communications, 2001, , 115-116.	4.1	49
176	Novel pH-Reporter MRI Contrast Agents. Angewandte Chemie, 2002, 114, 4510-4512.	2.0	49
177	Molecular Dynamics Simulation of [Gd(egta)(H2O)]â^' in Aqueous Solution: Internal Motions of the Poly(amino carboxylate) and Water Ligands, and Rotational Correlation Times. Chemistry - A European Journal, 2002, 8, 1031.	3.3	49
178	Tuning the Coordination Number of Hydroxypyridonate-Based Gadolinium Complexes:Â Implications for MRI Contrast Agents1. Journal of the American Chemical Society, 2006, 128, 5344-5345.	13.7	49
179	Maximizing the relaxivity of HSA-bound gadolinium complexes by simultaneous optimization of rotation and water exchange. Chemical Communications, 2007, , 4726.	4.1	49
180	Bifunctional ligands based on the DOTA-monoamide cage. Organic and Biomolecular Chemistry, 2008, 6, 1176.	2.8	49

#	Article	IF	CITATIONS
181	Dual MRI-SPECT agent for pH-mapping. Chemical Communications, 2011, 47, 1539-1541.	4.1	49
182	Equilibrium, Kinetic and Structural Studies of AAZTA Complexes with Ga <sup>3+</sup> , In <sup>3+</sup> and Cu <sup>2+</sup> . European Journal of Inorganic Chemistry, 2013, 2013, 147-162.	2.0	49
183	Quantification of hydroxyl exchange of Dâ€Clucose at physiological conditions for optimization of glucoCEST MRI at 3, 7 and 9.4 Tesla. NMR in Biomedicine, 2019, 32, e4113.	2.8	49
184	Metabolic Studies of Tumor Cells Using [1â€ <sup>13</sup> C] Pyruvate Hyperpolarized by Means of PHIPâ€Side Arm Hydrogenation. ChemPhysChem, 2019, 20, 318-325.	2.1	49
185	Dynamic 13C NMR spectroscopy of metal carbonyls. Progress in Nuclear Magnetic Resonance Spectroscopy, 1977, 11, 183-210.	7.5	48
186	1H and 17O-NMR relaxometric investigations of paramagnetic contrast agents for MRI. Clues for higher relaxivities. Coordination Chemistry Reviews, 1999, 185-186, 321-333.	18.8	48
187	Efficient relaxivity enhancement in dendritic gadolinium complexes: effective motional coupling in medium molecular weight conjugates. Chemical Communications, 2005, , 474.	4.1	48
188	A Quantitative Relaxometric Version of the ELISA Test for the Measurement of Cell Surface Biomarkers. Angewandte Chemie - International Edition, 2014, 53, 3488-3491.	13.8	48
189	Hyperpolarization transfer from parahydrogen to deuterium via carbon-13. Journal of Chemical Physics, 2003, 119, 8890-8896.	3.0	47
190	Advances in Metal-Based Probes for MR Molecular Imaging Applications. Current Medicinal Chemistry, 2010, 17, 3684-3700.	2.4	47
191	Synthesis and Characterization of a Hypoxia‣ensitive MRI Probe. Chemistry - A European Journal, 2012, 18, 9669-9676.	3.3	47
192	On the Fate of MRI Gd-Based Contrast Agents in Cells. Evidence for Extensive Degradation of Linear Complexes upon Endosomal Internalization. Analytical Chemistry, 2013, 85, 5627-5631.	6.5	47
193	Lanthanide-Loaded Erythrocytes As Highly Sensitive Chemical Exchange Saturation Transfer MRI Contrast Agents. Journal of the American Chemical Society, 2014, 136, 638-641.	13.7	47
194	Emerging Technologies to Image Tissue Metabolism. Cell Metabolism, 2019, 29, 518-538.	16.2	47
195	Relationships between structure and ligand dynamics. Journal of Organometallic Chemistry, 1989, 365, 163-185.	1.8	46
196	Neural-cell adhesion molecule (NCAM) expression by immature and tumor-derived endothelial cells favors cell organization into capillary-like structures. Experimental Cell Research, 2006, 312, 913-924.	2.6	46
197	Fe(III)-Templated Gd(III) Self-AssembliesA New Route toward Macromolecular MRI Contrast Agents1. Journal of the American Chemical Society, 2006, 128, 9272-9273.	13.7	46
198	First <i>exâ€vivo</i> MRI coâ€localization of two LIPOCEST agents. Contrast Media and Molecular Imaging, 2008, 3, 38-43.	0.8	46

42

#	Article	IF	CITATIONS
199	Exofacial Protein Thiols as a Route for the Internalization of Gd(III)-Based Complexes for Magnetic Resonance Imaging Cell Labeling. Journal of Medicinal Chemistry, 2010, 53, 4877-4890.	6.4	46
200	High-field oxygen-17 NMR spectroscopy: solution structures and dynamics of oxygen-17 enriched dodecacarbonyltetracobalt and dodecacarbonylhydroiron dicobaltate. Journal of the American Chemical Society, 1981, 103, 5920-5922.	13.7	45
201	Role of Osâ °H-Â-Â-Hâ °N Interactions in Directing the Stereochemistry of Carbonyl Cluster Hydride Derivatives. Organometallics, 1997, 16, 5140-5141.	2.3	45
202	Contrast Agents for Magnetic Resonance Imaging: A Novel Route to Enhanced Relaxivities Based on the Interaction of a GdIII Chelate with Poly-β-cyclodextrins. Chemistry - A European Journal, 1999, 5, 1253-1260.	3.3	45
203	Design of PLGA Based Nanoparticles for Imaging Guided Applications. Molecular Pharmaceutics, 2014, 11, 4100-4106.	4.6	45
204	Synthesis, X-ray Structure, and Solution NMR Studies of Ln(III) Complexes with a Macrocyclic Asymmetric Compartmental Schiff Base. Preference of the Ln(III) Ions for a Crown-Like Coordination Site. Inorganic Chemistry, 1999, 38, 2906-2916.	4.0	44
205	6-Carboxamido-5,4-Hydroxypyrimidinones:Â A New Class of Heterocyclic Ligands and Their Evaluation as Gadolinium Chelating Agents. Inorganic Chemistry, 2001, 40, 6746-6756.	4.0	44
206	Relaxometric and solution NMR structural studies on ditopic lanthanide(iii) complexes of a phosphinate analogue of DOTA with a fast rate of water exchange. Dalton Transactions, 2006, , 2323.	3.3	44
207	Gadolinium-binding cyclic hexapeptoids: synthesis and relaxometric properties. Organic and Biomolecular Chemistry, 2014, 12, 424-431.	2.8	44
208	Evidence for the Role of Intracellular Water Lifetime as a Tumour Biomarker Obtained by Inâ€Vivo Field ycling Relaxometry. Angewandte Chemie - International Edition, 2018, 57, 7468-7472.	13.8	44
209	The Issue of Gadolinium Retained in Tissues. Investigative Radiology, 2018, 53, 167-172.	6.2	44
210	Nuclear magnetic resonance studies of neutral lanthanide(III) complexes with tetraaza-macrocyclic ligands containing three phosphinate and one carboxamide co-ordinating arms. Journal of the Chemical Society Dalton Transactions, 1995, , 2259.	1.1	43
211	Melanin-Based Contrast Agents for Biomedical Optoacoustic Imaging and Theranostic Applications. International Journal of Molecular Sciences, 2017, 18, 1719.	4.1	43
212	Reactions of 3-hexyne with cobalt and iron carbonyls. Crystal structure and fluxionality of FeCo2(CO)9C2Et2. Inorganic Chemistry, 1982, 21, 501-505.	4.0	42
213	The alkyne-cluster interaction: structural, theoretical and mechanistic studies on the M2M'(CO)9(.mu.3eta.2-alkyne) complex (M = Fe; M' = Fe and Ru). Organometallics, 1984, 3, 1510-1515.	2.3	42
214	Solution structure and dynamics of DTPA-Ln(III) complexes (DTPA=diethylene triamine penta acetate;) Tj ETQq0 (	0 0 rgBT /C 2.4	)verlock 10 Tr
215	Azide, cyanide, fluoride, imidazole and pyridine binding to ferric and ferrous native horse heart cytochrome c and to its carboxymethylated derivative: A comparative study. Journal of Inorganic Biochemistry, 1996, 62, 213-222.	3.5	42

Isolation and 13C-NMR characterization of an insoluble proteinaceous fraction from substantia nigra of patients with parkinson's disease. Movement Disorders, 2000, 15, 977-981.
3.9

#	Article	IF	CITATIONS
217	NMR Structure of Two Novel Polyethylene Glycol Conjugates of the Human Growth Hormone-Releasing Factor, hGRF(1â~29)â~'NH2. Journal of the American Chemical Society, 2003, 125, 3458-3470.	13.7	42
218	Polarization transfer from para-hydrogen to heteronuclei: Effect of H/D substitution. The case of AA′X and spin systems. Journal of Magnetic Resonance, 2006, 178, 184-192.	2.1	42
219	New cyclodextrin dimers and trimers capable of forming supramolecular adducts with shape-specific ligands. Organic and Biomolecular Chemistry, 2009, 7, 370-379.	2.8	42
220	A novel patient-derived tumorgraft model with TRAF1-ALK anaplastic large-cell lymphoma translocation. Leukemia, 2015, 29, 1390-1401.	7.2	42
221	Synthesis, reactivity, and ligand dynamics of Ru3(CO)9(.muCO)(.mu.3eta.2-alkyne) compounds. Organometallics, 1991, 10, 2854-2856.	2.3	41
222	Structure and relaxivity of macrocyclic gadolinium complexes incorporating pyridyl and 4-morpholinopyridyl substituents. New Journal of Chemistry, 1999, 23, 669.	2.8	41
223	Conjugates of cyclodextrins with charged and neutral macrocyclic europium, terbium and gadolinium complexes: sensitised luminescence and relaxometric investigations and an example of supramolecular relaxivity enhancement. Perkin Transactions II RSC, 2000, , 1329-1338.	1.1	41
224	A Calix[4]arene GdIII Complex Endowed with High Stability, Relaxivity, and Binding Affinity to Serum Albumin. Angewandte Chemie - International Edition, 2001, 40, 4737-4739.	13.8	41
225	Synthesis of a carborane-containing cholesterol derivative and evaluation as a potential dual agent for MRI/BNCT applications. Organic and Biomolecular Chemistry, 2014, 12, 2457-2467.	2.8	41
226	In Vitro and In Vivo Assessment of Nonionic Iodinated Radiographic Molecules as Chemical Exchange Saturation Transfer Magnetic Resonance Imaging Tumor Perfusion Agents. Investigative Radiology, 2016, 51, 155-162.	6.2	41
227	Gd-AAZTA-MADEC, an improved blood pool agent for DCE-MRI studies on mice on 1ÂT scanners. Biomaterials, 2016, 75, 47-57.	11.4	41
228	Noninvasive evaluation of renal pH homeostasis after ischemia reperfusion injury by CESTâ€MRI. NMR in Biomedicine, 2017, 30, e3720.	2.8	41
229	Eight-Coordinate, Stable Fe(II) Complex as a Dual <sup>19</sup> F and CEST Contrast Agent for Ratiometric pH Imaging. Inorganic Chemistry, 2017, 56, 12206-12213.	4.0	41
230	Endogenous glutamine decrease is associated with pancreatic cancer progression. Oncotarget, 2017, 8, 95361-95376.	1.8	41
231	Dynamic properties of the trinuclear carbonyl cluster FeCo2(CO)95S and its derivatives. Inorganica Chimica Acta, 1977, 25, 103-108.	2.4	40
232	A Novel Application of para H2:Â the Reversible Addition/Elimination of H2at a Ru3Cluster Revealed by the Enhanced NMR Emission Resonance from Molecular Hydrogen. Journal of Physical Chemistry A, 1999, 103, 9702-9705.	2.5	40
233	Evidence for a Glycidic‣ipidic Matrix in Human Neuromelanin, Potentially Responsible for the Enhanced Iron Sequestering Ability of Substantia Nigra. Journal of Neurochemistry, 1994, 62, 369-371.	3.9	40
234	1,2-Hydroxypyridonate/Terephthalamide Complexes of Gadolinium(III): Synthesis, Stability, Relaxivity, and Water Exchange Properties. Inorganic Chemistry, 2009, 48, 277-286.	4.0	40

#	Article	IF	CITATIONS
235	The Role of Equilibrium and Kinetic Properties in the Dissociation of Gd[DTPAâ€bis(methylamide)] (Omniscan) at near to Physiological Conditions. Chemistry - A European Journal, 2015, 21, 4789-4799.	3.3	40
236	LipoCEST and cellCEST imaging agents: opportunities and challenges. Wiley Interdisciplinary Reviews: Nanomedicine and Nanobiotechnology, 2016, 8, 602-618.	6.1	40
237	Theranostic Nanoparticles Loaded with Imaging Probes and Rubrocurcumin for Combined Cancer Therapy by Folate Receptor Targeting. ChemMedChem, 2017, 12, 502-509.	3.2	40
238	An examination of the unsaturation in the clusters Fe4(CO)11(.mu.4-PR)2. Organometallics, 1986, 5, 245-252.	2.3	39
239	Molecular Recognition of R- and T-States of Human Adult Hemoglobin by a Paramagnetic Gd(III) Complex by Means of the Measurement of Solvent Water Proton Relaxation Rate. Journal of the American Chemical Society, 1995, 117, 9365-9366.	13.7	39
240	Hetero-Tripodal Hydroxypyridonate Gadolinium Complexes:Â Syntheses, Relaxometric Properties, Water Exchange Dynamics, and Human Serum Albumin Binding1. Inorganic Chemistry, 2004, 43, 8577-8586.	4.0	39
241	New Insights for Pursuing High Relaxivity MRI Agents from Modelling the Binding Interaction of GdIII Chelates to HSA. ChemBioChem, 2005, 6, 818-820.	2.6	39
242	Optimized Relaxivity and Stability of [Gd(H(2,2)-1,2-HOPO)(H2O)]-for Use as an MRI Contrast Agent1. Inorganic Chemistry, 2007, 46, 4796-4798.	4.0	39
243	High-relaxivity supramolecular aggregates containing peptides and Gd complexes as contrast agents in MRI. Journal of Biological Inorganic Chemistry, 2007, 12, 267-276.	2.6	39
244	The release of Doxorubicin from liposomes monitored by MRI and triggered by a combination of US stimuli led to a complete tumor regression in a breast cancer mouse model. Journal of Controlled Release, 2016, 230, 57-63.	9.9	39
245	Regiospecific substitution of trialkylphosphines for carbon monoxide in hydridoorganoruthenium clusters. Inorganic Chemistry, 1980, 19, 1571-1575.	4.0	38
246	MRI Contrast agents: macrocyclic lanthanide(III) complexes with improved relaxation efficiency. Journal of the Chemical Society Chemical Communications, 1995, , 1885.	2.0	38
247	Highly shifted LIPOCEST agents based on the encapsulation of neutral polynuclear paramagnetic shift reagents. Chemical Communications, 2008, , 600-602.	4.1	38
248	Lanthanide(III) Complexes of Tris(amide) PCTA Derivatives as Potential Bimodal Magnetic Resonance and Optical Imaging Agents. Chemistry - A European Journal, 2009, 15, 13188-13200.	3.3	38
249	<sup>15</sup> N Magnetic Resonance Hyperpolarization via the Reaction of Parahydrogen with <sup>15</sup> N-Propargylcholine. Journal of the American Chemical Society, 2012, 134, 11146-11152.	13.7	38
250	A Gadolinium(III) Zeolite-like Metal-Organic-Framework-Based Magnetic Resonance Thermometer. CheM, 2019, 5, 1609-1618.	11.7	38
251	Nanocarriers as Magic Bullets in the Treatment of Leukemia. Nanomaterials, 2020, 10, 276.	4.1	38
252	Reactivity of the ruthenium carbonyl hydride HRu3(CO)9C2C(CH3)3. Inorganica Chimica Acta, 1978, 26, 223-226.	2.4	37

#	Article	IF	CITATIONS
253	CO activation in the reactions of iron carbonyls and alkynes. Syntheses, crystal structures, and nuclear magnetic resonance studies on hydroxyferrole and maleoyliron derivatives. Journal of the Chemical Society Dalton Transactions, 1979, , 1664.	1.1	37
254	Synthesis, structure, and ligand dynamics of (.mu.,H)(.mu.3eta.2-CH3C=NCH2CH3)Ru3(CO)9. Organometallics, 1987, 6, 2074-2078.	2.3	37
255	A holmium complex of a macrocyclic ligand (DOTA) and its isostructural europium analogue. Acta Crystallographica Section C: Crystal Structure Communications, 1999, 55, 353-356.	0.4	37
256	Novel radical-responsive MRI contrast agent based on paramagnetic liposomes. Magnetic Resonance in Chemistry, 2003, 41, 585-588.	1.9	37
257	Gd loading by hypotonic swelling: an efficient and safe route for cellular labeling. Contrast Media and Molecular Imaging, 2013, 8, 475-486.	0.8	37
258	Polydopamine-decorated tobacco mosaic virus for photoacoustic/magnetic resonance bimodal imaging and photothermal cancer therapy. Nanoscale, 2019, 11, 9760-9768.	5.6	37
259	Hyperpolarized agents for advanced MRI investigations. Quarterly Journal of Nuclear Medicine and Molecular Imaging, 2009, 53, 604-17.	0.7	37
260	Multinuclear magnetic resonance studies. Part 2. Diphosphanes and dithioxodi-λ5-phosphanes. Journal of the Chemical Society Dalton Transactions, 1976, , 2144-2153.	1.1	36
261	Trinuclear osmium and ruthenium clusters containing ligands formed by dehydration and rearrangement of 1,4-dihydroxybut-2-yne. Inorganic Chemistry, 1981, 20, 2027-2031.	4.0	36
262	The alkyne-cluster interaction: structural, theoretical, and spectroscopic study on the parallel .mu.3eta.2 bonding mode in trinuclear carbonyl clusters of ruthenium and osmium. Inorganic Chemistry, 1986, 25, 4004-4010.	4.0	36
263	Synthesis and characterization of a Gd(iii) based contrast agent responsive to thiol containing compounds. Dalton Transactions, 2007, , 4980.	3.3	36
264	Evidence for <i>in vivo</i> macrophage mediated tumor uptake of paramagnetic/fluorescent liposomes. NMR in Biomedicine, 2009, 22, 1084-1092.	2.8	36
265	Reduction/Dissolution of a βâ€MnOOH Nanophase in the Ferritin Cavity To Yield a Highly Sensitive, Biologically Compatible Magnetic Resonance Imaging Agent. Angewandte Chemie - International Edition, 2010, 49, 612-615.	13.8	36
266	An MRI Method To Map Tumor Hypoxia Using Red Blood Cells Loaded with a pO <sub>2</sub> -Responsive Gd-Agent. ACS Nano, 2015, 9, 8239-8248.	14.6	36
267	A global view of standards for open image data formats and repositories. Nature Methods, 2021, 18, 1440-1446.	19.0	36
268	UV-PES, carbon-13 NMR and theoretical studies on the alkyne-cluster interaction in Fe3(CO)9(.mu.3eta.2-EtC2Et). Organometallics, 1983, 2, 430-434.	2.3	35
269	Synthesis and characterization of a novel DTPA-like gadolinium(III) complex: a potential reagent for the determination of glycated proteins by water proton NMR relaxation measurements. Inorganic Chemistry, 1993, 32, 2068-2071.	4.0	35
270	Innovative magnetic resonance imaging diagnostic agents based on paramagnetic Gd(III) complexes. Biopolymers, 2002, 66, 419-428.	2.4	35

#	Article	IF	CITATIONS
271	Relaxometric Investigations and MRI Evaluation of a Liposome-Loaded pH-Responsive Gadolinium(III) Complex. Inorganic Chemistry, 2012, 51, 7210-7217.	4.0	35
272	A vaccine targeting angiomotin induces an antibody response which alters tumor vessel permeability and hampers the growth of established tumors. Angiogenesis, 2012, 15, 305-316.	7.2	35
273	13C NMR study of methynyltricobalt enneacarbonyls. Inorganica Chimica Acta, 1976, 18, 9-11.	2.4	34
274	Relaxometric Studies for Food Characterization: The Case of Balsamic and Traditional Balsamic Vinegars. Journal of Agricultural and Food Chemistry, 2009, 57, 3028-3032.	5.2	34
275	Variation of water exchange dynamics with ligand structure and stereochemistry in lanthanide complexes based on 1,4-diazepine derivatives. Organic and Biomolecular Chemistry, 2009, 7, 1120.	2.8	34
276	Mnâ€loaded apoferritin: a highly sensitive MRI imaging probe for the detection and characterization of hepatocarcinoma lesions in a transgenic mouse model. Contrast Media and Molecular Imaging, 2012, 7, 281-288.	0.8	34
277	MRI evaluation of the antitumor activity of paramagnetic liposomes loaded with prednisolone phosphate. European Journal of Pharmaceutical Sciences, 2012, 45, 436-441.	4.0	34
278	B25716/1: a novel albumin-binding Gd-AAZTA MRI contrast agent with improved properties in tumor imaging. Journal of Biological Inorganic Chemistry, 2014, 19, 715-726.	2.6	34
279	Cluster analysis of quantitative parametric maps from DCE-MRI: application in evaluating heterogeneity of tumor response to antiangiogenic treatment. Magnetic Resonance Imaging, 2015, 33, 725-736.	1.8	34
280	Hydrogenative-PHIP polarized metabolites for biological studies. Magnetic Resonance Materials in Physics, Biology, and Medicine, 2021, 34, 25-47.	2.0	34
281	Relaxometric characterization of human hemalbumin. Journal of Biological Inorganic Chemistry, 2001, 6, 650-658.	2.6	33
282	1H and17O relaxometric investigations of the binding of Mn(II) ion to human serum albumin. Magnetic Resonance in Chemistry, 2002, 40, 41-48.	1.9	33
283	Characterization of human hair melanin and its degradation products by means of magnetic resonance techniques. Magnetic Resonance in Chemistry, 2008, 46, 471-479.	1.9	33
284	Synthesis of Gd(III)-C-palmitamidomethyl-Câ€2-DOTAMA-C6-o-carborane: a new dual agent for innovative MRI/BNCT applications. Organic and Biomolecular Chemistry, 2008, 6, 4460.	2.8	33
285	Release of Toxic Gd <sup>3+</sup> Ions to Tumour Cells by Vitaminâ€B <sub>12</sub> Bioconjugates. Chemistry - A European Journal, 2009, 15, 7980-7989.	3.3	33
286	Re-evaluation of the water exchange lifetime value across red blood cell membrane. Biochimica Et Biophysica Acta - Biomembranes, 2016, 1858, 627-631.	2.6	33
287	Rare earth elements (REE) in biology and medicine. Rendiconti Lincei, 2020, 31, 821-833.	2.2	33
288	Synthesis and reactivity of trinuclear osmium and dinuclear and trinuclear ruthenium compounds derived from hydroxyalkynes. Journal of the Chemical Society Dalton Transactions, 1981, , 828.	1.1	32

#	Article	IF	CITATIONS
289	Synthesis, NMR, relaxometry and circularly polarised luminescence studies of macrocyclic monoamidetris(phosphinate) complexes bearing a remote chiral centre. Journal of the Chemical Society Dalton Transactions, 1998, , 881-892.	1.1	32
290	The Effect of Ligand Scaffold Size on the Stability of Tripodal Hydroxypyridonate Gadolinium Complexes. Inorganic Chemistry, 2003, 42, 2577-2583.	4.0	32
291	Magnetic resonance imaging visualization of targeted cells by the internalization of supramolecular adducts formed between avidin and biotinylated Gd3+ chelates. Journal of Biological Inorganic Chemistry, 2005, 10, 78-86.	2.6	32
292	Catalytic effects of apoferritin interior surface residues on water proton exchange in lanthanide complexes. Contrast Media and Molecular Imaging, 2006, 1, 10-14.	0.8	32
293	A Carboraneâ€Derivative "Click―Reaction under Heterogeneous Conditions for the Synthesis of a Promising Lipophilic MRI/GdBNCT Agent. Chemistry - A European Journal, 2013, 19, 721-728.	3.3	32
294	NMR investigation of the equilibrium partitioning of a water-soluble bile salt protein carrier to phospholipid vesicles. Proteins: Structure, Function and Bioinformatics, 2013, 81, 1776-1791.	2.6	32
295	Chemical Insights into the Issues of Gd Retention in the Brain and Other Tissues Upon the Administration of Gdâ€Containing MRI Contrast Agents. European Journal of Inorganic Chemistry, 2019, 2019, 137-151.	2.0	32
296	Nuclear magnetic relaxation dispersion profiles of substantia nigra pars compacta in Parkinson's disease patients are consistent with protein aggregation. Neurochemistry International, 2000, 37, 331-336.	3.8	31
297	New paramagnetic supramolecular adducts for MRI applications based on non-covalent interactions between Gd(III)-complexes and β- or γ-cyclodextrin units anchored to chitosan. Journal of Inorganic Biochemistry, 2006, 100, 931-938.	3.5	31
298	Efficient Cellular Labeling by CD44 Receptorâ€Mediated Uptake of Cationic Liposomes Functionalized with MRI Contrast Agents. ChemMedChem, 2008, 3, 1858-1862.	3.2	31
299	Yeast cell wall particles: a promising class of nature-inspired microcarriers for multimodal imaging. Chemical Communications, 2011, 47, 10635.	4.1	31
300	Gadolinium-doped LipoCEST agents: a potential novel class of dual 1H-MRI probes. Chemical Communications, 2011, 47, 4667.	4.1	31
301	Combined inhibition of PI3Kβ and PI3Kγ reduces fat mass by enhancing α-MSH–dependent sympathetic drive. Science Signaling, 2014, 7, ra110.	3.6	31
302	Ferritin Decorated PLGA/Paclitaxel Loaded Nanoparticles Endowed with an Enhanced Toxicity Toward MCF-7 Breast Tumor Cells. Bioconjugate Chemistry, 2017, 28, 1283-1290.	3.6	31
303	Water Soluble Melanin Derivatives for Dynamic Contrast Enhanced Photoacoustic Imaging of Tumor Vasculature and Response to Antiangiogenic Therapy. Advanced Healthcare Materials, 2017, 6, 1600550.	7.6	31
304	A <i>R</i> <sub>2p</sub> / <i>R</i> <sub>1p</sub> Ratiometric Procedure to Assess Matrix Metalloproteinaseâ€2 Activity by Magnetic Resonance Imaging. Angewandte Chemie - International Edition, 2013, 52, 3926-3930.	13.8	30
305	Highly Shifted Proton MR Imaging: Cell Tracking by Using Direct Detection of Paramagnetic Compounds. Radiology, 2014, 272, 785-795.	7.3	30
306	Products of the reaction of Ru3(CO)12 with 1,3-cyclohexadiene. X-ray structure of (Îbenzene)nonacarbonyl-1-cyclohexen-1,2-ylenetetraruthenium, Ru4(CO)9(C6H6)(C6H8). Inorganica Chimica Acta, 1979, 34, 49-55.	2.4	29

Silvio Aime

#	Article	IF	CITATIONS
307	Acid-induced Isomerisations of osmium and ruthenium clusters involving hydroxide transfer from carbon to metal atoms. X-Ray crystal structure of nonacarbonyl-µ3-(3,3-diphenylallene-) Tj ETQq1 1 0.784314 r Transactions, 1982, , 1625-1629.	gBT /Overl 1.1	ock 10 Tf 50
308	Paramagnetic GdIIIî—,FeIII heterobimetallic complexes of DTPA-bis-salicylamide. Spectrochimica Acta Part A: Molecular Spectroscopy, 1993, 49, 1315-1322.	0.1	29
309	Relaxometric Determination of the Exchange Rate of the Coordinated Water Protons in a Neutral Gd <sup>III</sup> Chelate. Chemistry - A European Journal, 1997, 3, 1499-1504.	3.3	29
310	Improved syntheses of bis(β-cyclodextrin) derivatives, new carriers for gadolinium complexes. Organic and Biomolecular Chemistry, 2006, 4, 1124.	2.8	29
311	An unusual gadolinium ten-coordinated dimeric complex in the series of MRI contrast agents: Na[Gd(H2O)AAZTA]·3H2O. Inorganica Chimica Acta, 2008, 361, 1534-1541.	2.4	29
312	Gd-loaded-RBCs for the assessment of tumor vascular volume byÂcontrast-enhanced-MRI. Biomaterials, 2015, 58, 82-92.	11.4	29
313	High kinetic inertness of a bis-hydrated Gd-complex with a constrained AAZTA-like ligand. Chemical Communications, 2016, 52, 11235-11238.	4.1	29
314	Carbon-hydrogen bond activation in novel cyclopentadienyl acetylenic carbonyl clusters of iron, ruthenium and nickel. Inorganica Chimica Acta, 1978, 30, 9-12.	2.4	28
315	Relationships between structure and ligand dynamics in organometal clusters. Organometallics, 1982, 1, 640-644.	2.3	28
316	Unsymmetrically substituted furoxans. VII. A <sup>13</sup> C NMR study of a series of isomeric pairs of furoxans and the structure of the two isomeric chloroâ€phenylâ€furoxans. Journal of Heterocyclic Chemistry, 1982, 19, 427-430.	2.6	28
317	NMR Studies of Melanins: Characterization of a Soluble Melanin Free Acid From Sepia Ink. Pigment Cell & Melanoma Research, 1991, 4, 216-221.	3.6	28
318	Coordination of an Imine Ligand on an Os3 Cluster Stabilized by Intramolecular Osâ^'HHâ^'N Hydrogen Bonding. Organometallics, 1999, 18, 2030-2032.	2.3	28
319	NOVEL PARAMAGNETIC MACROMOLECULAR COMPLEXES DERIVED FROM THE LINKAGE OF A MACROCYCLIC Gd(III) COMPLEX TO POLYAMINO ACIDS THROUGH A SQUARIC ACID MOIETY. Bioconjugate Chemistry, 1999, 10, 701-701.	3.6	28
320	Well-Defined, Multifunctional Nanostructures of a Paramagnetic Lipid and a Lipopeptide for Macrophage Imaging. Journal of the American Chemical Society, 2009, 131, 406-407.	13.7	28
321	αâ€ŧrideuteromethyl[15N]glutamine: A longâ€ŀived hyperpolarized perfusion marker. Magnetic Resonance in Medicine, 2016, 76, 1900-1904.	3.0	28
322	Nano-sized and other improved reporters for magnetic resonance imaging of angiogenesis. Advanced Drug Delivery Reviews, 2017, 119, 61-72.	13.7	28
323	Singlet ontrast Magnetic Resonance Imaging: Unlocking Hyperpolarization with Metabolism**. Angewandte Chemie - International Edition, 2021, 60, 6791-6798.	13.8	28
324	Reactions of alkynes with HFeCO3(CO)12. Crystal structure of FeCO3(CO)9[PhC2(H)Ph] (PhC2Ph). Inorganica Chimica Acta, 1983, 71, 141-147.	2.4	27

#	Article	IF	CITATIONS
325	13C solid State MAS NMR spectra of [M3(CO)12] complexes (M = Ru and Os). Evidence for motional effects in [Ru3(CO)12]. Inorganica Chimica Acta, 1988, 146, 151-152.	2.4	27
326	Structural and Spectroscopic Study of the Dihydrogen Bond in an Imine Triosmium Complex. Organometallics, 2002, 21, 50-57.	2.3	27
327	Cardio-Chemical Exchange Saturation Transfer Magnetic Resonance Imaging Reveals Molecular Signatures of Endogenous Fibrosis and Exogenous Contrast Media. Circulation: Cardiovascular Imaging, 2015, 8, .	2.6	27
328	An innovative therapeutic approach for malignant mesothelioma treatment based on the use of Gd/boron multimodal probes for MRI guided BNCT. Journal of Controlled Release, 2018, 280, 31-38.	9.9	27
329	Crystal structure and stereochemical non-rigidity of octacarbonyl-(Î1,3-dimethyl-2-vinylcyclopentadienyl)-µ3-propylidyne-triangulo-tri-iron. Journal of the Chemical Society Dalton Transactions, 1977, , 227-232.	1.1	26
330	Lanthanide-Loaded Paramagnetic Liposomes as Switchable Magnetically Oriented Nanovesicles. Inorganic Chemistry, 2008, 47, 2928-2930.	4.0	26
331	Evaluation of <sup>111</sup> In-Labeled EPep and FibPep as Tracers for Fibrin SPECT Imaging. Molecular Pharmaceutics, 2013, 10, 4309-4321.	4.6	26
332	Chemical exchange saturation transfer (CEST): an efficient tool for detecting molecular information on proteins' behaviour. Analyst, The, 2014, 139, 2687-2690.	3.5	26
333	Simultaneous MR imaging for tissue engineering in a rat model of stroke. Scientific Reports, 2015, 5, 14597.	3.3	26
334	Mesoporous silica nanoparticles functionalized with fluorescent and MRI reporters for the visualization of murine tumors overexpressing α <sub>v</sub> l² <sub>3</sub> receptors. Nanoscale, 2016, 8, 7094-7104.	5.6	26
335	CESTâ€MRI for glioma pH quantification in mouse model: Validation by immunohistochemistry. NMR in Biomedicine, 2018, 31, e4005.	2.8	26
336	170 NMR spectroscopy of transition metal carbonyls. Journal of Organometallic Chemistry, 1979, 178, 171-175.	1.8	25
337	Ligand Dynamics in H2Os3(CO)10 and H2Os3(CO)10L. Journal of Organometallic Chemistry, 1981, 213, 207-213.	1.8	25
338	NOE (Nuclear Overhauser Effect) Transfers frompara-H2Enhanced Magnetizations in Alkene Moieties at Rh(I) Centers. Journal of Physical Chemistry A, 2001, 105, 6305-6310.	2.5	25
339	The Water-Exchange Rate in Neutral Heptadentate DO3A-Like GdIII Complexes: Effect of the Basicity at the Macrocyclic Nitrogen Site. European Journal of Inorganic Chemistry, 2003, 2003, 3530-3533.	2.0	25
340	The crystallized solvent could influence the lanthanide water bonding?. Inorganica Chimica Acta, 2006, 359, 3405-3411.	2.4	25
341	Photochemical activation of endosomal escape of MRIâ€Gdâ€agents in tumor cells. Magnetic Resonance in Medicine, 2011, 65, 212-219.	3.0	25
342	Relaxometric Study of a Series of Monoaqua Gd <sup>III</sup> Complexes of Rigidified EGTAâ€Like Chelators and Their Noncovalent Interaction with Human Serum Albumin. European Journal of Inorganic Chemistry, 2011, 2011, 802-810.	2.0	25

#	Article	IF	CITATIONS
343	Boronated Compounds for Imaging Guided BNCT Applications. Anti-Cancer Agents in Medicinal Chemistry, 2012, 12, 543-553.	1.7	25
344	Mn loaded apoferritin as an MRI sensor of melanin formation in melanoma cells. Chemical Communications, 2012, 48, 2436.	4.1	25
345	High Relaxivity Supramolecular Adducts Between Humanâ€Liver Fattyâ€Acidâ€Binding Protein and Amphiphilic Gd <sup>III</sup> Complexes: Structural Basis for the Design of Intracellular Targeting MRI Probes. Chemistry - A European Journal, 2012, 18, 9919-9928.	3.3	25
346	EXCI-CEST: Exploiting pharmaceutical excipients as MRI-CEST contrast agents for tumor imaging. International Journal of Pharmaceutics, 2017, 525, 275-281.	5.2	25
347	In-vitro NMR Studies of Prostate Tumor Cell Metabolism by Means of Hyperpolarized [1-13C]Pyruvate Obtained Using the PHIP-SAH Method. Frontiers in Oncology, 2020, 10, 497.	2.8	25
348	Agents for Polarization Enhancement in MRI. Handbook of Experimental Pharmacology, 2008, , 247-272.	1.8	25
349	Reaction of 4-methylpent-2-yne with dodecacarbonyltriruthenium. The structure of a novel alkyne dimerization dehydrogenation product. Journal of the Chemical Society Dalton Transactions, 1981, , 2023.	1.1	24
350	Intramolecular nucleophilic attack at the α-carbon atom of a µ3-alkynyl ligand in a triosmium cluster. Journal of the Chemical Society Dalton Transactions, 1983, , 1807-1809.	1.1	24
351	Dynamic processes in the solid state. Proton relaxation studies and potential energy barrier calculations for (arene)M(CO)3 species. X-ray crystal structures of (1,2,3-C6H3Me3)Cr(CO)3 and (1,2,4,5-C6H2Me4)Cr(CO)3. Inorganic Chemistry, 1991, 30, 951-956.	4.0	24
352	Chapter 8 considerations on high resolution solid state NMR in paramagnetic molecules. Coordination Chemistry Reviews, 1996, 150, 221-242.	18.8	24
353	A paramagnetic probe to localize residues next to carboxylates on protein surfaces. Journal of Biological Inorganic Chemistry, 2002, 7, 617-622.	2.6	24
354	Enantioselective Recognition between Chiral α-Hydroxyâ^'Carboxylates and Macrocyclic Heptadentate Lanthanide(III) Chelates. Inorganic Chemistry, 2003, 42, 4891-4897.	4.0	24
355	A Novel Method of Cellular Labeling: Anchoring MRâ€Imaging Reporter Particles on the Outer Cell Surface. ChemMedChem, 2008, 3, 60-62.	3.2	24
356	Block copolymer vesicles containing paramagnetic lanthanide complexes: a novel class of T1- and CEST MRI contrast agents. Soft Matter, 2010, 6, 4847.	2.7	24
357	MRI Paramagnetic Probes for Cellular Labeling. European Journal of Inorganic Chemistry, 2012, 2012, 1934-1944.	2.0	24
358	Frequency-Encoded MRI-CEST Agents Based on Paramagnetic Liposomes/RBC Aggregates. Nano Letters, 2014, 14, 6857-6862.	9.1	24
359	Synthesis and spectroscopic characterization of heterobimetallic (α-alkynyl)iron-cobalt hexacarbonyl complexes, μ-(1-σ, 2-3, η2-R2C-CCR′)][(CO)3Fe-Co(CO)3] and [μ-(1-σ, 2-3, η2-H2C-CCCH2OH)] [(CO)3Fe-Co(CO)2(PPh3)]. Polyhedron, 1983, 2, 77-81.	2.2	23
360	Molecular structures and dynamic behaviour of two isomers of [Ru3(µ-H)(µ3-Me2NC4H4)(CO)9] formed from 1-dimethylaminobut-2-yne and containing η2-alkene-1,3-diyl and η2-alkene-1,2-diyl ligands respectively. Journal of the Chemical Society Dalton Transactions, 1986, , 1459-1463.	1.1	23

#	Article	IF	CITATIONS
361	Use of solid-state carbon-13 NMR spectroscopy to quantify the degree of asymmetry of bonding for semibridging carbonyl groups in iron carbonyl complexes. Inorganic Chemistry, 1991, 30, 1489-1493.	4.0	23
362	Reactivity Studies of Para-Hydrogen with μ3-Quinolyl Triosmium Clusters. Organometallics, 2002, 21, 1508-1511.	2.3	23
363	Peptide Derivatized Lamellar Aggregates as Target-Specific MRI Contrast Agents. ChemBioChem, 2007, 8, 950-955.	2.6	23
364	Synthesis and solution thermodynamic study of rigidified and functionalised EGTA derivatives. Organic and Biomolecular Chemistry, 2008, 6, 2361.	2.8	23
365	Chemistry of Molecular Imaging. Accounts of Chemical Research, 2009, 42, 821-821.	15.6	23
366	How to design <sup>13</sup> C <i>para</i> â€hydrogenâ€induced polarization experiments for MRI applications. Contrast Media and Molecular Imaging, 2011, 6, 77-84.	0.8	23
367	Novel Gd(III)â€based probes for MR molecular imaging of matrix metalloproteinases. Contrast Media and Molecular Imaging, 2012, 7, 175-184.	0.8	23
368	<sup>15</sup> Nâ€ <i>P</i> ermethylated amino acids as efficient probes for MRIâ€DNP applications. Contrast Media and Molecular Imaging, 2013, 8, 417-421.	0.8	23
369	Towards a Successful Clinical Implementation of Fluorescence-Guided Surgery. Molecular Imaging and Biology, 2014, 16, 147-151.	2.6	23
370	Gd accumulation in tissues of healthy mice upon repeated administrations of Gadodiamide and Gadoteridol. Journal of Trace Elements in Medicine and Biology, 2018, 48, 239-245.	3.0	23
371	Exploiting the Proton Exchange as an Additional Route to Enhance the Relaxivity of Paramagnetic MRI Contrast Agents. Inorganic Chemistry, 2018, 57, 5567-5574.	4.0	23
372	Absence of dentate nucleus restingâ€state functional connectivity changes in nonneurological patients with gadoliniumâ€related hyperintensity on T <sub>1</sub> â€weighted images. Journal of Magnetic Resonance Imaging, 2019, 50, 445-455.	3.4	23
373	Synthesis, crystal structure, and stereochemical non-rigidity of $\hat{A}\mu$ -[1- $\hat{I}f$ :1 $\hat{a}\in$ <sup>4</sup> 2- $\hat{i}$ -2-carboxylato-1-ethylbut-1-enyl-O(2Fe)]-bis(tricarbonyl-iron)(Fe $\hat{a}\in$ <sup>4</sup> Fe), a new complex obtained from iron carbonyls under apolar conditions. Journal of the Chemical Society Dalton Transactions, 1979 1155-1159	1.1	22
374	Carbon–nitrogen bond cleavage in 1-dimethylaminobut-2-yne and derived ligands in triruthenium and triosmium clusters. Journal of the Chemical Society Dalton Transactions, 1984, , 1987.	1.1	22
375	High-field magic-angle-spinning carbon-13 NMR spectroscopy of tetracobalt dodecacarbonyl. Inorganic Chemistry, 1989, 28, 1196-1198.	4.0	22
376	Trends in NMR studies of paramagnetic Gd(III) complexes as potential contrast agents in MRI. Magnetic Resonance Imaging, 1991, 9, 843-847.	1.8	22
377	Solution Structures and Dynamics of Ru4(.muH)4(CO)12-xLx (x = 1-4, L = P(OEt)3, PPh3; x = 1-2, L =) Tj ETQq1 2 Ru4(.muH)4(CO)10(P(OEt)3)2. Organometallics, 1995, 14, 3693-3703.	l 0.78431 2.3	4 rgBT /Ove 22
378	Novel MRI and fluorescent probes responsive to the Factor XIII transglutaminase activity. Contrast Media and Molecular Imaging, 2010, 5, 213-222.	0.8	22

#	Article	lF	CITATIONS
379	Target Visualization by MRI Using the Avidin/Biotin Amplification Route: Synthesis and Testing of a Biotin–Gdâ€DOTA Monoamide Trimer. Chemistry - A European Journal, 2010, 16, 8080-8087.	3.3	22
380	MRI of cells and mice at 1 and 7 Tesla with Gdâ€ŧargeting agents: when the low field is better!. Contrast Media and Molecular Imaging, 2011, 6, 421-425.	0.8	22
381	Successful Entrapping of Liposomes in Glucan Particles: An Innovative Micron-Sized Carrier to Deliver Water-Soluble Molecules. Molecular Pharmaceutics, 2014, 11, 3760-3765.	4.6	22
382	Assessing tumor vascularization as a potential biomarker of imatinib resistance in gastrointestinal stromal tumors by dynamic contrast-enhanced magnetic resonance imaging. Gastric Cancer, 2017, 20, 629-639.	5.3	22
383	Fe(deferasirox) <sub>2</sub> : An Iron(III)-Based Magnetic Resonance Imaging <i>T</i> <sub>1</sub> Contrast Agent Endowed with Remarkable Molecular and Functional Characteristics. Journal of the American Chemical Society, 2021, 143, 14178-14188.	13.7	22
384	Electronic structure of ferracyclopentadienyl derivatives. UV PES ab initio study of Fe2(.muCO)(CO)5(C4R4) and Fe3(.muCO)2(CO)6(C4R4). Inorganic Chemistry, 1985, 24, 1241-1246.	4.0	21
385	Water signal suppression by T2-relaxation enhancement promoted by Dy(III) complexes. Magnetic Resonance in Chemistry, 1991, 29, S85-S88.	1.9	21
386	Solid-Gas Reactions of the "Lightly Stabilized" Os3(CO)11L (L = NCCH3, C2H4) Clusters with CO, NH3, and H2. Organometallics, 1995, 14, 3224-3228.	2.3	21
387	Synthesis and Characterization of Triosmium Clusters Containing the Bidentate Ligand Ph2PCH2CH2SMe:  Detection of an Isomerization Reaction Involving Bridging and Chelating Ligand Coordination Modes. Organometallics, 2001, 20, 4150-4160.	2.3	21
388	Heterodinuclear LnNa Complexes with an Asymmetric Macrocyclic Compartmental Schiff Base. Chemistry - A European Journal, 2002, 8, 3917-3926.	3.3	21
389	Lanthanide-Loaded Paramagnetic Liposomes as Switchable Magnetically Oriented Nanovesicles. Methods in Enzymology, 2009, 464, 193-210.	1.0	21
390	SPECT imaging of fibrin using fibrinâ€binding peptides. Contrast Media and Molecular Imaging, 2013, 8, 229-237.	0.8	21
391	Synthesis and Relaxometric Characterization of a MRI Gd-Based Probe Responsive to Glutamic Acid Decarboxylase Enzymatic Activity. Journal of Medicinal Chemistry, 2013, 56, 2466-2477.	6.4	21
392	Paramagnetic Phospholipid-Based Micelles Targeting VCAM-1 Receptors for MRI Visualization of Inflammation. Bioconjugate Chemistry, 2016, 27, 1921-1930.	3.6	21
393	Macrocyclic paramagnetic agents for MRI: Determinants of relaxivity and strategies for their improvement. Magnetic Resonance in Medicine, 2017, 78, 1523-1532.	3.0	21
394	Targeting Chronic Myeloid Leukemia Stem/Progenitor Cells Using Venetoclax-Loaded Immunoliposome. Cancers, 2021, 13, 1311.	3.7	21
395	Carbon-13 nuclear magnetic resonance spectra of σ,Îbinuclear complexes prepared from dodecacarbonyltri-iron and acetylenes. Journal of the Chemical Society Dalton Transactions, 1976, , 838-840.	1.1	20
396	Solution structures and dynamics of Co4(CO)12 and HFeCo3(CO)12â^'xLx (x = 0–3; L = group V Ligand). Inorganica Chimica Acta, 1978, 30, 45-49.	2.4	20

#	Article	IF	CITATIONS
397	Solution structure and dynamics of H2Ru4(CO)13. Inorganica Chimica Acta, 1978, 29, L211-L212.	2.4	20
398	Multinuclear n.m.r. studies of transition metal carbonyl clusters. Inorganica Chimica Acta, 1982, 62, 51-56.	2.4	20
399	Note. Two-dimensional nuclear magnetic resonance for the analysis of the carbon-13 spectra of carbonyl groups in metallocarbonyls. Journal of the Chemical Society Dalton Transactions, 1985, , 225.	1.1	20
400	A New Class of Contrast Agents for Magnetic Resonance Imaging Based on Selective Reduction of Water-T2 by Chemical Exchange. Investigative Radiology, 1988, 23, S267-S270.	6.2	20
401	Metal ion content in Sepia officinalis melanin. Marine Chemistry, 1992, 39, 243-250.	2.3	20
402	Spectral Discrimination of Chiral Macrocyclic Paramagnetic Metal Complexes by NMR Techniquesâ‰. Chemistry - A European Journal, 1999, 5, 1261-1266.	3.3	20
403	Investigating Pathways of Molecular H2 Exchange in (μ-H)2Os3(CO)10. Organometallics, 2001, 20, 2924-2927.	2.3	20
404	Synthesis of the Gd(III) complex with a tetrazole-armed macrocyclic ligand as a potential MRI contrast agent. Tetrahedron Letters, 2002, 43, 783-786.	1.4	20
405	Targeting exofacial protein thiols with GdIII complexes. An efficient procedure for MRI cell labelling. Chemical Communications, 2009, , 893.	4.1	20
406	Design and testing of paramagnetic liposome-based CEST agents for MRI visualization of payload release on pH-induced and ultrasound stimulation. Journal of Biological Inorganic Chemistry, 2014, 19, 207-214.	2.6	20
407	Crystal and molecular structure of Ru3(CO)6(C12H20CO)(C12H20): an example of four alkynic groups bonded to a metal cluster. Inorganica Chimica Acta, 1978, 27, 145-151.	2.4	19
408	Kinetic deuterium isotope effects on .muhydride and carbonyl ligand migrations. Organometallics, 1984, 3, 1790-1795.	2.3	19
409	Synthesis, structure, and isomerisation of triruthenium and triosmium clusters derived from 3-dimethylaminoprop-1-yne; X-ray crystal structure of [Ru3–H(CO)9(Me2N+–CH2)]. Journal of the Chemical Society Dalton Transactions, 1984, , 1981-1986.	1.1	19
410	1H and 13C NMR Study of the Solid-State Dynamics of H4Ru4(CO)12. Organometallics, 1994, 13, 2375-2379.	2.3	19
411	Synthesis, crystal structure and solid-state dynamics of the La(hfa)3·Me(OCH2CH2)4OMe (Hhfaâ€=â€1,1,1,5,5,5-hexafluoropentane-2,4-dione) precursor for MOCVD applications. Journal of the Chemical Society Dalton Transactions, 1998, , 1509-1512.	1.1	19
412	?-Cyclodextrin adducts of Gd(III) chelates: useful models for investigating the structural and dynamic determinants of the relaxivity of gadolinium-based systems. Magnetic Resonance in Chemistry, 2003, 41, 800-805.	1.9	19
413	HR-MAS of cells: A "cellular water shift―due to water-protein interactions?. Magnetic Resonance in Medicine, 2005, 54, 1547-1552.	3.0	19
414	Blast from the Past: The Aluminums Ghost on the Lanthanum Salts. Current Medicinal Chemistry, 2005, 12, 1631-1636.	2.4	19

#	Article	IF	CITATIONS
415	para-Hydrogenation of unsaturated moieties on poly(lysine) derived substrates for the development of novel hyperpolarized MRI contrast agents. Organic and Biomolecular Chemistry, 2005, 3, 3948.	2.8	19
416	New CD derivatives as self-assembling contrast agents for magnetic resonance imaging (MRI). Journal of Inclusion Phenomena and Macrocyclic Chemistry, 2007, 57, 489-495.	1.6	19
417	Tuning Glutamine Binding Modes in Gdâ€ÐOTAâ€Based Probes for an Improved MRI Visualization of Tumor Cells. Chemistry - A European Journal, 2009, 15, 76-85.	3.3	19
418	Assessment of iron absorption in mice by ICP-MS measurements of 57Fe levels. European Journal of Nutrition, 2012, 51, 783-789.	3.9	19
419	MRI nanoprobes based on chemical exchange saturation transfer: Ln <sup>III</sup> chelates anchored on the surface of mesoporous silica nanoparticles. Nanoscale, 2014, 6, 9604-9607.	5.6	19
420	<scp>MRI</scp> <scp>CEST</scp> at 1 <scp>T</scp> with large µ <sub>eff</sub> <scp>L</scp> n <sup>3+</sup> complexes <scp>T</scp> m <sup>3+</sup> â€ <scp>HPDO</scp> 3 <scp>A</scp> : An efficient <scp>MRI</scp> p <scp>H</scp> reporter. Magnetic Resonance in Medicine, 2016, 75, 329-336.	3.0	19
421	Enzymeâ€Responsive LipoCEST Agents: Assessment of MMPâ€2 Activity by Measuring the Intraâ€liposomal Water <sup>1</sup> Hâ€NMR Shift. Angewandte Chemie - International Edition, 2017, 56, 12170-12173.	13.8	19
422	Complete on/off responsive ParaCEST MRI contrast agents for copper and zinc. Dalton Transactions, 2018, 47, 11346-11357.	3.3	19
423	L-ferritin: A theranostic agent of natural origin for MRI visualization and treatment of breast cancer. Journal of Controlled Release, 2020, 319, 300-310.	9.9	19
424	UV photoelectron and theoretical studies of organometal carbonyl clusters of ruthenium and osmiummuHydridomu.3-alkynyl triangulo cluster compounds. Inorganic Chemistry, 1983, 22, 744-748.	4.0	18
425	An inspection into the class of bis(alkyne)-undecacarbonyl-quadro-tetraruthenium complexes. Crystal structure and dynamic behaviour of Ru4(CO)11 (μ4, η2-MeC2Ph)2. Inorganica Chimica Acta, 1984, 85, 161-168.	2.4	18
426	Solution structures and dynamics of M3(CO)12â^'x(NCCH3)x (Mî—»Ru, x = 1, 2, 3; Mî—»Os, x = 1, 2). Inorganica Chimica Acta, 1995, 235, 357-366.	2.4	18
427	Metal Complexes as Allosteric Effectors of Human Hemoglobin: An NMR Study of the Interaction of the Gadolinium(III) Bis(m-boroxyphenylamide)diethylenetriaminepentaacetic Acid Complex with Human Oxygenated and Deoxygenated Hemoglobin. Biophysical Journal, 1999, 76, 2735-2743.	0.5	18
428	Mannich Reaction as a New Route to Pyridine-Based Polyaminocarboxylic Ligands. Organic Letters, 2004, 6, 1201-1204.	4.6	18
429	Solution Structure of the Supramolecular Adduct between a Liver Cytosolic Bile Acid Binding Protein and a Bile Acid-Based Gadolinium(III)-Chelate, a Potential Hepatospecific Magnetic Resonance Imaging Contrast Agent. Journal of Medicinal Chemistry, 2008, 51, 6782-6792.	6.4	18
430	In vivo MRI visualization of release from liposomes triggered by local application of pulsed low-intensity non-focused ultrasound. Nanomedicine: Nanotechnology, Biology, and Medicine, 2014, 10, e901-e904.	3.3	18
431	Synthesis of High Relaxivity Gadolinium AAZTA Tetramers as Building Blocks for Bioconjugation. Bioconjugate Chemistry, 2018, 29, 1428-1437.	3.6	18
432	Nitrogen derivatives of iron carbonyls. Part 5. New routes in the mechanism of reaction of dodecacarbonyl-triangulo-tri-iron with nitro-alkanes, and X-ray analysis of µ-[acetone oximato(1—)-NO]-µ-isopropyl-amido-bis(tricarbonyliron)(Fe–Fe). Journal of the Chemical Society Dalton Transactions, 1978, , 534-540.	1.1	17

#	Article	IF	CITATIONS
433	Reactions of protic acids with a hydridoorganometal cluster: HRu3(CO)9(C2C(CH3)3). Inorganic Chemistry, 1981, 20, 1592-1597.	4.0	17
434	Activation of the Mî—,CO bond in transition metal complexes. CO substitution reactions in di-, tri- and tetra-nuclear metal carbonyl compounds catalyzed by [Fe(CO)2(η5-C5H5)]2. Inorganica Chimica Acta, 1986, 115, 129-133.	2.4	17
435	Reactions of Solid H2Os3(CO)10 with Gaseous CO, NH3, and H2S. Organometallics, 1994, 13, 4232-4236.	2.3	17
436	Paramagnetic complexes as novel NMR pH indicators. Chemical Communications, 1996, , 1265.	4.1	17
437	Determination of the Prototropic Exchange Rate at the Water Molecule Coordinated to an Anionic Paramagnetic GdIII Chelate. European Journal of Inorganic Chemistry, 1998, 1998, 1283-1289.	2.0	17
438	Binding and Relaxometric Properties of Heme Complexes with Cyanogen Bromide Fragments of Human Serum Albumin. Biophysical Journal, 2002, 83, 2248-2258.	0.5	17
439	Separation of intra- and extracellular lactate NMR signals using a lanthanide shift reagent. Magnetic Resonance in Medicine, 2002, 47, 10-13.	3.0	17
440	Advisory about gadolinium calls for caution in the treatment of uremic patients with lanthanum carbonate. Kidney International, 2007, 72, 1162-1163.	5.2	17
441	NMR Structural Studies of the Supramolecular Adducts between a Liver Cytosolic Bile Acid Binding Protein and Gadolinium(III)-Chelates Bearing Bile Acids Residues:  Molecular Determinants of the Binding of a Hepatospecific Magnetic Resonance Imaging Contrast Agent. Journal of Medicinal Chemistry. 2007. 50. 5257-5268.	6.4	17
442	The effects of intramolecular H-bond formation on the stability constant and water exchange rate of the Gd(III)-diethylenetriamine-N′-(3-amino-1,1-propylenephosphonic)-N,N,N″,N″-tetraacetate complex. Contrast Media and Molecular Imaging, 2007, 2, 94-102.	0.8	17
443	Molecular recognition of sugars by lanthanide (III) complexes of a conjugate of <i>N, N</i> â€bis[2â€{bis[2â€{1, 1â€dimethylethoxy)â€2â€oxoethyl]amino]ethyl]glycine and phenylboronic acid. Cont Media and Molecular Imaging, 2007, 2, 163-171.	tra9t8	17
444	Targeting of human renal tumor-derived endothelial cells with peptides obtained by phage display. Journal of Molecular Medicine, 2007, 85, 897-906.	3.9	17
445	In Vivo Labeling of B16 Melanoma Tumor Xenograft with a Thiol-Reactive Gadolinium Based MRI Contrast Agent. Molecular Pharmaceutics, 2011, 8, 1750-1756.	4.6	17
446	Structure-Function Relationships of Iodinated Contrast Media and Risk of Nephrotoxicity. Current Medicinal Chemistry, 2012, 19, 736-743.	2.4	17
447	In vivo imaging of inhibitory, GABAergic neurons by MRI. NeuroImage, 2012, 62, 1685-1693.	4.2	17
448	Design and Synthesis of a γ <sup>1</sup> β <sup>8</sup> yclodextrin Oligomer: A New Platform with Potential Application as a Dendrimeric Multicarrier. Chemistry - A European Journal, 2013, 19, 12086-12092.	3.3	17
449	Assessing the transport rate of hyperpolarized pyruvate and lactate from the intra- to the extracellular space. NMR in Biomedicine, 2016, 29, 1022-1027.	2.8	17
450	Intramolecular motion in tetra-t-butyldiphosphine. Journal of the Chemical Society Chemical Communications, 1974, , 426.	2.0	16

#	Article	IF	CITATIONS
451	A 13C Nmr investigation of stereochemical non rigidity in hydrido olefinic carbonyl clusters of ruthenium. Inorganica Chimica Acta, 1976, 20, 217-220.	2.4	16
452	Carbon–carbon σ-bond cleavage in α-hydroxyalkynes on reaction with dodecacarbonyl-triosmium and -triruthenium. Journal of the Chemical Society Chemical Communications, 1980, , 1168-1169.	2.0	16
453	Reaction of Ru3(CO)12 with styrene. Journal of Organometallic Chemistry, 1982, 233, 247-252.	1.8	16
454	Oxygen-17 and carbon-13 relaxation studies of metal carbonyls: improved determination of 17O electric quadrupole couplings. Journal of the Chemical Society Dalton Transactions, 1984, , 1863.	1.1	16
455	Oximation of acetyl(hydroxyimino)acetone: nuclear magnetic resonance spectroscopic, chemical, and X-ray crystallographic studies of the reaction products. Journal of the Chemical Society Perkin Transactions II, 1987, , 523.	0.9	16
456	Paramagnetic water proton relaxation enhancement: From contrast agents in MRI to reagents for quantitative "in vitro―assays. Magnetic Resonance Imaging, 1992, 10, 849-854.	1.8	16
457	Relationship between Solid State NMR Parameters and X-ray Structural Data in Tricadmium Phosphates. Inorganic Chemistry, 1996, 35, 149-154.	4.0	16
458	Novel Synthesis, Solution Structure, Dynamics, and Protonation of H(μ-H)Ru3(CO)11. Organometallics, 1998, 17, 3182-3185.	2.3	16
459	Improving the relaxivity by dimerizing Gd-AAZTA: Insights for enhancing the sensitivity of MRI contrast agents. Inorganic Chemistry Communication, 2010, 13, 663-665.	3.9	16
460	Synthesis and Physicochemical Characterization of Carbon Backbone Modified [Gd(TTDA)(H2O)]2â^'Derivatives. Inorganic Chemistry, 2011, 50, 1275-1287.	4.0	16
461	MRI Tracking of Macrophages Labeled with Glucan Particles Entrapping a Water Insoluble Paramagnetic Gd-Based Agent. Molecular Imaging and Biology, 2013, 15, 307-315.	2.6	16
462	Inâ€Vivo Magnetic Resonance Imaging Detection of Paramagnetic Liposomes Loaded with Amphiphilic Gadolinium(III) Complexes: Impact of Molecular Structure on Relaxivity and Excretion Efficiency. ChemPlusChem, 2013, 78, 712-722.	2.8	16
463	Novel Gastrin-Releasing Peptide Receptor Targeted Near-Infrared Fluorescence Dye for Image-Guided Surgery of Prostate Cancer. Molecular Imaging and Biology, 2020, 22, 85-93.	2.6	16
464	In vivo assessment of tumour associated macrophages in murine melanoma obtained by low-field relaxometry in the presence of iron oxide particles. Biomaterials, 2020, 236, 119805.	11.4	16
465	Dynamic properties and solution structures of the clusters [Fe3(CO)9X2](X = S, Se, Te, or NMe) and their derivatives. Journal of the Chemical Society Dalton Transactions, 1980, , 46.	1.1	15
466	13Cî—,13C coupling constants in μ2- and μ4-(η2-acetylene) complexes of cobalt. Journal of Organometallic Chemistry, 1984, 262, c1-c4.	1.8	15
467	Solution dynamics of the osmium cluster [Os3(µ-H)2(CO)10] by13C and17O nuclear magnetic resonance. Estimation of the13C chemical shift anisotropy and17O quadrupole coupling constant. Journal of the Chemical Society Dalton Transactions, 1984, , 279-284.	1.1	15
468	Dynamic behavior of the flyover bridge complexes M2(CO)5L {.mu[C(R):C(R')]2CO} (M = Ru, Fe; L = CO,) Tj ET	Qq <u>0 0</u> 0 rş	gBT_/Overlock

#	Article	IF	CITATIONS
469	The reaction of Co4(CO)12 with Ph2PCH2CH2PPh2. Spectroscopic identification of polymeric products. Journal of Organometallic Chemistry, 1986, 309, C51-C55.	1.8	15
470	Bis(diphenylphosphino)methane-substituted products from (μ3-CCH3)Co3(CO)9. Journal of Organometallic Chemistry, 1987, 320, 229-237.	1.8	15
471	Proton spin-lattice NMR relaxation studies of hydride carbonyl clusters: a method to evaluate distances involving hydrido ligands. Inorganic Chemistry, 1991, 30, 1614-1617.	4.0	15
472	Stabilization of the T-state of ferrous human adult and fetal hemoglobin by Ln(III) complexes: A thermodynamic study. Journal of Inorganic Biochemistry, 1998, 71, 37-43.	3.5	15
473	Detection of a novel intermediate in the addition of thiols to osmium carbonyl clusters. Chemical Communications, 1998, , 2721-2722.	4.1	15
474	An iron-based T 1 contrast agent made of iron-phosphate complexes: In vitro and in vivo studies. Magnetic Resonance Materials in Physics, Biology, and Medicine, 2007, 20, 27-37.	2.0	15
475	Insights on the relaxation of liposomes encapsulating paramagnetic Lnâ€based complexes. Magnetic Resonance in Medicine, 2015, 74, 468-473.	3.0	15
476	CESTâ€MRI studies of cells loaded with lanthanide shift reagents. Magnetic Resonance in Medicine, 2018, 80, 1626-1637.	3.0	15
477	Efficient Route to Label Mesenchymal Stromal Cell-Derived Extracellular Vesicles. ACS Omega, 2018, 3, 8097-8103.	3.5	15
478	Liposome-Based Bioassays. Biology, 2020, 9, 202.	2.8	15
479	Observation of localised CO exchange mechanisms at the iron and ruthenium centres of di-µ-carbonyl (Fe : Ru2, Ru3)-di-µ-hydrido (Ru1: Ru2,) Tj ETQq1 1 0.784314 rgBT /Overlock 10 Tf 50 342 Td (Ru3)-tetrahedro Journal of the Chemical Society Chemical Communications, 1975, , 452-454.	-tris(tricar 2.0	boŋylruthenii
480	Stereochemically non rigid acetylenic carbonyl complexes of iron and cobalt. Inorganica Chimica Acta, 1976, 16, L7-L8.	2.4	14
481	Two-dimensional nuclear magnetic resonance for the quantitative analysis of three-site exchange in the ruthenium cluster [Ru3(14-H)(CO)9(MeCCHCme)]. Journal of Magnetic Resonance, 1985, 65, 173-177.	0.5	14
482	Mechanism of localized site exchange of carbonyl groups in HM3(CO)9L clusters. Inorganic Chemistry, 1985, 24, 231-233.	4.0	14
483	13C solid state CP/MAS NMR studies of EDTA complexes. Inorganica Chimica Acta, 1987, 129, L23-L25.	2.4	14
484	NMR Relaxometric Investigation on Human Methemoglobin and Fluoromethemoglobin. An Improved Quantitativein Vitro Assay of Human Methemoglobin. Magnetic Resonance in Medicine, 1995, 33, 827-831.	3.0	14
485	Evaluation of the energy barrier for carbonyl exchange in the highly fluxional Ru3(CO)12 system. Organometallics, 1995, 14, 4435-4438.	2.3	14
486	NMR characterization of four new isomers of H(μ-H)Os3(CO)10(phosphine). Inorganica Chimica Acta, 1998, 275-276, 521-527.	2.4	14

#	Article	IF	CITATIONS
487	Ring-opening polymerisation of norbornene by (μ-H)2Os3(CO)10 complex. Journal of Organometallic Chemistry, 2001, 622, 43-46.	1.8	14
488	One-step synthesis of a new eight-membered cyclic ligand from glycine, formaldehyde and hypophosphorous acid. Tetrahedron Letters, 2002, 43, 8387-8389.	1.4	14
489	Magnetic resonance imaging of tumor cells by targeting the amino acid transport system. Bioorganic and Medicinal Chemistry Letters, 2006, 16, 4111-4114.	2.2	14
490	Gd-enhanced MR images of substrates other than water. Contrast Media and Molecular Imaging, 2006, 1, 101-105.	0.8	14
491	1H and 17O NMR relaxometric study in aqueous solution of Gd(III) complexes of EGTA-like derivatives bearing methylenephosphonic groups. Magnetic Resonance in Chemistry, 2008, 46, S86-S93.	1.9	14
492	Contrast agents and mechanisms. Drug Discovery Today: Technologies, 2011, 8, e109-e115.	4.0	14
493	Supramolecular protamine/Gd-loaded liposomes adducts as relaxometric protease responsive probes. Bioorganic and Medicinal Chemistry, 2011, 19, 1131-1135.	3.0	14
494	Release of a Paramagnetic Magnetic Resonance Imaging Agent from Liposomes Triggered by Low Intensity Non-Focused Ultrasound. Journal of Medical Imaging and Health Informatics, 2013, 3, 356-366.	0.3	14
495	Role of the reaction intermediates in determining PHIP (parahydrogen induced polarization) effect in the hydrogenation of acetylene dicarboxylic acid with the complex [Rh (dppb)]+ (dppb:) Tj ETQq1 1 0.784314 r	gBT3 <b>/O</b> ver	lock140 Tf 50
496	A rigidified AAZTA-like ligand as efficient chelator for68Ga radiopharmaceuticals. ChemistrySelect, 2016, 1, 163-171.	1.5	14
497	Gadolinium presence, MRI hyperintensities, and glucose uptake in the hypoperfused rat brain after repeated administrations of gadodiamide. Neuroradiology, 2019, 61, 163-173.	2.2	14
498	Chalcogen derivatives of iron carbonyls. X. Reaction Mechanism of the CO substitution on Fe2(CO)6(μX)2(X = S, Se) with ligands. Inorganica Chimica Acta, 1980, 40, 131-140.	2.4	13
499	Gas-phase helium(He I) photoelectron spectra of methinyltricobalt enneacarbonyl clusters. Inorganic Chemistry, 1982, 21, 1081-1084.	4.0	13
500	Carbonî—,halogen bond activation at Ru3(CO)12. Journal of Organometallic Chemistry, 1983, 244, C47-C49.	1.8	13
501	UV photoelectron and theoretical studies of organometal carbonyl clusters of ruthenium and osmiummuHydridomu.3-allyl and .muhydridomu.3-allenyl triangulo cluster compounds. Inorganic Chemistry, 1985, 24, 570-575.	4.0	13
502	NMR studies of the reorientational motions of cyclopentadienyl ligands in solidcis- andtrans-[(η5-C5H5)2Fe2(CO)2(μ2-CO)2]. Magnetic Resonance in Chemistry, 1990, 28, S52-S58.	1.9	13
503	Hetero-dinuclear sodium–lanthanide(iii) complexes with an asymmetric compartmental macrocycle. Chemical Communications, 2000, , 145-146.	4.1	13
504	Slow clearance gadolinium-based extracellular and intravascular contrast media for three-dimensional MR angiography. Journal of Magnetic Resonance Imaging, 2001, 13, 588-593.	3.4	13

#	Article	IF	CITATIONS
505	NMR Conformational Analysis of Antide, a Potent Antagonist of the Gonadotropin Releasing Hormone. Journal of the American Chemical Society, 2002, 124, 3431-3442.	13.7	13
506	187Os subspectra in1H and31P{1H} spectra of triosmium carbonyl clusters. Magnetic Resonance in Chemistry, 2002, 40, 107-113.	1.9	13
507	Detection and Quantification of Lanthanide Complexes in Cell Lysates by Matrix-Assisted Laser Desorption/Ionization Time-of-Flight Mass Spectrometry. Analytical Chemistry, 2004, 76, 6012-6016.	6.5	13
508	Water exchange across the erythrocyte plasma membrane studied by HR-MAS NMR spectroscopy. Magnetic Resonance in Medicine, 2006, 56, 978-985.	3.0	13
509	Effect of a mesityleneâ€based ligand cap on the relaxometric properties of Gd(III) hydroxypyridonate MRI contrast agents. Contrast Media and Molecular Imaging, 2009, 4, 220-229.	0.8	13
510	MRI Contrast Agents for Pharmacological Research. Frontiers in Pharmacology, 2015, 6, 290.	3.5	13
511	Synthesis of phosphonic analogues of AAZTAâ€AAZTA=6-Amino-6-methylperhydro-1,4-diazepine-N,N′,N″,N″-tetraacetic acid.†and relaxometric evaluation of the corresponding Gd(III) complexes as potential MRI contrast agents. Tetrahedron Letters. 2015, 56, 1994-1997.	1.4	13
512	Exploring the intramolecular catalysis of the proton exchange process to modulate the relaxivity of Gd( <scp>iii</scp> )-complexes of HP-DO3A-like ligands. Chemical Communications, 2018, 54, 10056-10059.	4.1	13
513	Gadolinium Retention in Erythrocytes and Leukocytes From Human and Murine Blood Upon Treatment With Gadolinium-Based Contrast Agents for Magnetic Resonance Imaging. Investigative Radiology, 2020, 55, 30-37.	6.2	13
514	Contaminations in (meta)genome data: An open issue for the scientific community. IUBMB Life, 2020, 72, 698-705.	3.4	13
515	Relaxometric studies of erythrocyte suspensions infected by <i>Plasmodium falciparum</i> : a tool for staging infection and testing antiâ€malarial drugs. Magnetic Resonance in Medicine, 2020, 84, 3366-3378.	3.0	13
516	Synthesis and crystal structure of heptacarbonyl-Hydrido-(t-butylethynyl)-(2,4-hexadiene)-triangulo-triruthenium, HRu3(CO)7(C6H9)(C6H10). Inorganica Chimica Acta, 1979, 32, 163-169.	2.4	12
517	The structures and fluxional behaviour of the binary carbonyls; a new approach. Part 3. The fluxional behaviour of [Fe3(CO)11L], L = PR3 or P(OR)3. Journal of the Chemical Society Dalton Transactions, 1981, , 1535.	1.1	12
518	The alkyne-cluster interaction in a ruthenium "butterfly―acetylenic carbonyl complex. An UV-PES and theoretical study. Journal of Organometallic Chemistry, 1983, 244, 383-391.	1.8	12
519	Electrochemical investigation of a series of organotriruthenium clusters. Organometallics, 1984, 3, 1374-1378.	2.3	12
520	NMR study of the chemical exchange of the hydrido ligands in the bis(bis(diphenylphosphino)ethane)trihydridodiplatinum(II) cation by T1, T2, and HD isotopic perturbation. Inorganic Chemistry, 1991, 30, 316-318.	4.0	12
521	Magnetic resonance imaging of the gastrointestinal tract: Investigation of baby milk as a low cost contrast medium. European Journal of Radiology, 1992, 15, 171-174.	2.6	12
522	Reorientational motions of permethylated cyclopentadienyl rings in polycrystalline organometallic compounds. Inorganic Chemistry, 1992, 31, 3054-3059.	4.0	12

#	Article	IF	CITATIONS
523	Stereochemical Nonrigidity in (.mu.2-H)(H)Os3(CO)11. Evidence for the Occurrence of a Racemization Process at Low Temperature. Organometallics, 1994, 13, 3737-3739.	2.3	12
524	Multinuclear and multifrequency NMR study of gadolinium(III) complexes with bis-amide derivatives of ethylenedioxydiethylenedinitrilotetraacetic acid. Dalton Transactions RSC, 2000, , 3435-3440.	2.3	12
525	Gadolinium(III) Complexes of dota-DerivedN-Sulfonylacetamides (H4(dota-NHSO2R)=10-{2-[(R)sulfonylamino]-2-oxoethyl}-1,4,7,10-tetraazacyclododecane-1,4,7-triacetic) Tj ETG Chimica Acta. 2005. 88. 588-603.	Qq110.78	84314 rgBT /( 12
526	The use of contrast agents with fast field-cycling magnetic resonance imaging. Physics in Medicine and Biology, 2011, 56, 105-115.	3.0	12
527	Cancer cell death induced by ferritins and the peculiar role of their labile iron pool. Oncotarget, 2018, 9, 27974-27984.	1.8	12
528	Relaxometric investigations addressing the determination of intracellular water lifetime: a novel tumour biomarker of general applicability. Molecular Physics, 2019, 117, 968-974.	1.7	12
529	X-Ray molecular structure of Âμ-(isopropylamino)-Âμ-(propanone) Tj ETQq1 1 0.784314 rgBT /Overlock 10 Tf 50 of the Chemical Society Chemical Communications, 1976, .	507 Td (c 2.0	oximato-O,N)- 11
530	Cluster expansion reactions of HRu3(CO)9MeCî—1CHî—1CMe, a nido-Pentagonal-bipyramidal complex. Inorganica Chimica Acta, 1982, 57, 207-210.	2.4	11
531	Nuclear magnetic resonance of binuclear complexes containing a metallacyclopentadiene system. Journal of the Chemical Society Dalton Transactions, 1986, , 1863.	1.1	11
532	Notes. Carbon-13 and oxygen-17 nuclear magnetic resonance relaxation studies of [M3(CO)12] derivatives (M = Fe, Ru, or Os). Journal of the Chemical Society Dalton Transactions, 1988, , 791.	1.1	11
533	Solid-gas reactions of molecular organometallic complexes. Detection of a metastable intermediate in the carbonylation of a nickel(0) complex. Organometallics, 1993, 12, 4757-4763.	2.3	11
534	Coordination of Imines on Os3Clusters: Effect of the Solvent in Addressing Isomer Formation. Organometallics, 2000, 19, 707-710.	2.3	11
535	Modulation of the antioxidant activity of HO scavengers by albumin binding: a 19F-NMR study. Biochemical and Biophysical Research Communications, 2003, 307, 962-966.	2.1	11
536	Sensitive MRI detection of internalized <i>T</i> <sub>1</sub> contrast agents using magnetization transfer contrast. NMR in Biomedicine, 2015, 28, 1663-1670.	2.8	11
537	AAZTA: An Ideal Chelating Agent for the Development of <sup>44</sup> Sc PET Imaging Agents. Angewandte Chemie, 2017, 129, 2150-2154.	2.0	11
538	[Yb(AAZTA)(H <sub>2</sub> 0)] <sup>â^²</sup> : an unconventional ParaCEST MRI probe. Chemical Communications, 2018, 54, 2004-2007.	4.1	11
539	Modulation of the Prototropic Exchange Rate in pHâ€Responsive Ybâ€HPDO3A Derivatives as ParaCEST Agents. ChemistrySelect, 2018, 3, 6035-6041.	1.5	11
540	Lack of Plasma Protein Hemopexin Results in Increased Duodenal Iron Uptake. PLoS ONE, 2013, 8, e68146.	2.5	11

#	Article	IF	CITATIONS
541	Stoichiometric and catalytic hydrogenation of the [Co2(CO)6(μ2-η2-alkyne)] complexes. Inorganica Chimica Acta, 1985, 100, 97-105.	2.4	10
542	Proton NMR spin-lattice relaxation studies of hydridometal clusters of ruthenium and osmium. Inorganic Chemistry, 1987, 26, 2551-2552.	4.0	10
543	13C Solid-State Cross Polarization/Magic-Angle-Spinning Nuclear Magnetic Resonance Spectra of Natural and Synthetic Melanins. Pigment Cell & Melanoma Research, 1988, 1, 355-357.	3.6	10
544	Synthesis, molecular structure, crystal packing, and dynamic behaviour in the solid state of [Fe2(η5-C5H5)2(Âμ-CO)(CO)2{Âμ-CR(CN)}](R = H or CN). Journal of the Chemical Society Dalton Transactions, 1992, , 2961-2966.	1.1	10
545	H/D Isotopic Exchange on the Surface of a Triosmium Carbonyl Cluster. Organometallics, 1996, 15, 4967-4970.	2.3	10
546	The role of molecular shape and axial symmetry in the solid state molecular dynamics of metal carbonyl compounds included in cyclodextrin cavities. Dalton Transactions RSC, 2000, , 4075-4077.	2.3	10
547	Coordination equilibrium in an Ln(III) macrocyclic chelate modulated by a reversible interaction with a weakly donor substituent. Magnetic Resonance in Chemistry, 2002, 40, 87-92.	1.9	10
548	Effect of low and zero magnetic field on the hyperpolarization lifetime in parahydrogenated perdeuterated molecules. Journal of Magnetic Resonance, 2009, 200, 15-20.	2.1	10
549	Hyperpolarized13C-pyruvate magnetic resonance imaging in cancer diagnostics. Expert Opinion on Medical Diagnostics, 2012, 6, 335-345.	1.6	10
550	Hyperpolarized <sup>13</sup> Câ€labelled anhydrides as DNP precursors of metabolic MRI agents. Contrast Media and Molecular Imaging, 2012, 7, 469-477.	0.8	10
551	Evaluation of the dose enhancement of combined <sup>10</sup> B+ <sup>157</sup> Gd neutron capture therapy (NCT). Radiation Protection Dosimetry, 2015, 166, 369-373.	0.8	10
552	In Vivo MR Imaging of Fibrin in a Neuroblastoma Tumor Model by Means of a Targeting Gd-Containing Peptide. Molecular Imaging and Biology, 2015, 17, 819-828.	2.6	10
553	Unsaturated Longâ€Chain Fatty Acids Are Preferred Ferritin Ligands That Enhance Iron Biomineralization. Chemistry - A European Journal, 2017, 23, 9879-9887.	3.3	10
554	Tumor Targeting via Sialic Acid: [68Ga]DOTA-en-pba as a New Tool for Molecular Imaging of Cancer with PET. Molecular Imaging and Biology, 2018, 20, 798-807.	2.6	10
555	ParaHydrogen Polarized Ethylâ€{1â€ <sup>13</sup> C]pyruvate in Water, a Key Substrate for Fostering the PHIPâ€ <del>S</del> AH Approach to Metabolic Imaging. ChemPhysChem, 2021, 22, 1042-1048.	2.1	10
556	Effect of the hydrogenation solvent in the PHIP-SAH hyperpolarization of [1-13C]pyruvate. Catalysis Today, 2022, 397-399, 94-102.	4.4	10
557	Prospects and limitations of paramagnetic chemical exchange saturation transfer agents serving as biological reporters in vivo. NMR in Biomedicine, 2023, 36, e4698.	2.8	10
558	13C n.m.r. spectra of highly 13CO-enriched metal carbonyls: observation of 2 J cc cis coupling constants. Journal of the Chemical Society Chemical Communications, 1981, , 300.	2.0	9

#	Article	IF	CITATIONS
559	Triruthenium clusters containing dinethylamino-substituted allyl and allenyl ligands: The transmission of electronic substituent effects through clusters. Journal of Organometallic Chemistry, 1981, 214, C15-C18.	1.8	9
560	Theoretical and spectroscopic studies of (.mubutatriene)hexacarbonyldiiron compounds. Inorganic Chemistry, 1982, 21, 4073-4076.	4.0	9
561	Fluxional behaviour of the binary carbonyls. A comparison of the isoelectronic and isostructural tetranuclear clusters: Co4(CO)12, HFeCo3(CO)12 and[FeCo3(CO)12]â´. Inorganica Chimica Acta, 1983, 68, 141-145.	2.4	9
562	Carbon-metal hydrogen interchange in organometal clusters of ruthenium and osmium. Organometallics, 1988, 7, 856-858.	2.3	9
563	Factors Determining the Proton T1 Relaxivity in Solutions Containing Gd-DTPA. Investigative Radiology, 1988, 23, S264-S266.	6.2	9
564	An NMR study of the interaction between Melanin Free Acid and Mn2+ ions as a model to mimic the enhanced proton relaxation rates in melanotic melanoma. Magnetic Resonance Imaging, 1991, 9, 963-968.	1.8	9
565	NMR relaxometric studies of water accessibility to haem cavity in horse heart and sperm whale myoglobin. Magnetic Resonance in Chemistry, 1993, 31, S85-S89.	1.9	9
566	Solution and solid-state NMR studies of MeHgII and RSHgII (R = Me, Et) complexes with pyrazolyl-containing ligands. Polyhedron, 1994, 13, 2695-2702.	2.2	9
567	Fast carbonyl exchange in the solid state for β-cyclodextrin/(arene)Cr(CO)3 inclusion complexes. Chemical Communications, 1999, , 281-282.	4.1	9
568	An NMR Study of H(μ-H)Os3(CO)11. Inorganic Chemistry, 2000, 39, 2422-2425.	4.0	9
569	A novel non-facial mode of azulene cluster co-ordination. Crystal and molecular structure of the dicarbenoid Os3(μ-H)2(CO)9(μ3-η1â^¶Î·1â^¶Î·1-C10H6). Dalton Transactions RSC, 2000, , 2215-2217.	2.3	9
570	High Relaxivity Contrast Agents for MRI and Molecular Imaging. , 2005, , 99-121.		9
571	The Detection of PHIP Effects Allows New Insights into the Mechanism of Olefin Isomerisation during Catalytic Hydrogenation. European Journal of Inorganic Chemistry, 2008, 2008, 4348-4351.	2.0	9
572	Towards improved boron neutron capture therapy agents: evaluation of in vitro cellular uptake of a glutamine-functionalized carborane. Journal of Biological Inorganic Chemistry, 2009, 14, 883-890.	2.6	9
573	Optimizing the high-field relaxivity by self-assembling of macrocyclic Gd( <scp>iii</scp> ) complexes. Dalton Transactions, 2015, 44, 4910-4917.	3.3	9
574	Functional imaging of the angiogenic switch in a transgenic mouse model of human breast cancer by dynamic contrast enhanced magnetic resonance imaging. International Journal of Cancer, 2016, 139, 404-413.	5.1	9
575	Enhanced relaxivity of Gd <sup>III</sup> -complexes with HP-DO3A-like ligands upon the activation of the intramolecular catalysis of the prototropic exchange. Inorganic Chemistry Frontiers, 2021, 8, 1500-1510.	6.0	9
576	In vitro and in vivo comparison of MRI chemical exchange saturation transfer (CEST) properties between native glucose and 3â€Oâ€Methylâ€Dâ€glucose in a murine tumor model. NMR in Biomedicine, 2021, e4602.	342.8	9

#	Article	IF	CITATIONS
577	GlucoCEST MRI for the Evaluation Response to Chemotherapeutic and Metabolic Treatments in a Murine Triple-Negative Breast Cancer: A Comparison with[18F]F-FDG-PET. Molecular Imaging and Biology, 2022, 24, 126-134.	2.6	9
578	Visualization through magnetic resonance imaging of DNA internalized following "in vivo" electroporation. Molecular Imaging, 2005, 4, 7-17.	1.4	9
579	Reinvestigation of the solution structure of Co4(CO)12 by 13C and 59Co NMR. 2 Journal of Magnetic Resonance, 1985, 65, 308-315.	0.5	8
580	A new method for the determination of 17O electric quadrupole couplings. Terminal, bridging, and capping CO groups in metallocarbonyls. Journal of Magnetic Resonance, 1986, 68, 597-599.	0.5	8
581	Synthesis of the alkoxo(hydrido)-clusters [Ru3(µ-H)(CO)10(µ-OR)][R = Me, Et, Prn, or Bun] catalysed by dinuclear carbonyl iron complexes. Journal of the Chemical Society Dalton Transactions, 1987, , 253-254.	1.1	8
582	Solid state13C NMR spectra of metal carbonyl clusters. Journal of Cluster Science, 1993, 4, 1-8.	3.3	8
583	Modulation of the Prototropic Exchange Rate at the Water Molecule Coordinated to a GdIII Ion. European Journal of Inorganic Chemistry, 2003, 2003, 2045-2048.	2.0	8
584	Where have all the lanthanum salts gone, long time passing?. Kidney International, 2003, 64, 2327-2328.	5.2	8
585	Intramolecular Host–Guest Dynamics of FeCp(CO)2X (X = I and CH3) and Mo2Cp2(CO)6 Included in β- or γ-Cyclodextrin. European Journal of Inorganic Chemistry, 2008, 2008, 152-157.	2.0	8
586	Synthesis and Relaxometric Properties of Gadolinium(III) Complexes of New Triazineâ€Based Polydentate Ligands. Helvetica Chimica Acta, 2009, 92, 2414-2426.	1.6	8
587	Para-hydrogen induced polarization of Si-29 NMR resonances as a potentially useful tool for analytical applications. Magnetic Resonance in Chemistry, 2012, 50, 529-533.	1.9	8
588	Use of FCC-NMRD relaxometry for early detection and characterization of ex-vivo murine breast cancer. Scientific Reports, 2019, 9, 4624.	3.3	8
589	Differences in Molecular Structure Markedly Affect GBCA Elimination Behavior. Radiology, 2019, 291, 267-268.	7.3	8
590	Modifying LnHPDO3A Chelates for Improved <i>T</i> <sub>1</sub> and CEST MRI Applications. Chemistry - A European Journal, 2019, 25, 4184-4193.	3.3	8
591	An innovative approach for the synthesis of dual modality peptide imaging probes based on the native chemical ligation approach. Chemical Communications, 2020, 56, 3500-3503.	4.1	8
592	A Novel Class of 1 Hâ€MRI Contrast Agents Based on the Relaxation Enhancement Induced on Water Protons by 14 Nâ€Containing Imidazole Moieties. Angewandte Chemie - International Edition, 2021, 60, 4208-4214.	13.8	8
593	Detection of U-87 Tumor Cells by RGD-Functionalized/Gd-Containing Giant Unilamellar Vesicles in Magnetization Transfer Contrast Magnetic Resonance Images. Investigative Radiology, 2021, 56, 301-312.	6.2	8

594 Chapter 19 Iodinated Contrast Media as pH-Responsive CEST Agents. , 2017, , 447-466.

#	Article	IF	CITATIONS
595	Activation of alkynes by transition metals. Journal of the Chemical Society Chemical Communications, 1979, , 704.	2.0	7
596	Iron-57 satellites in 13C NMR spectra: an aid to elucidation of "hidden-processes―in the dynamics of metal carbonyls. Journal of Organometallic Chemistry, 1981, 214, C27-C30.	1.8	7
597	Complexes of diethylenetriaminepentaacetic acid as contrast agents in NMR imaging. Computer simulation of equilibria in human blood plasma. Analytica Chimica Acta, 1990, 233, 85-100.	5.4	7
598	A 13C CP/MAS NMR Study of the Structure and Dynamics of [(η5-C5H5)2Fe2(CO)4] Included in γ-Cyclodextrin:  Evidence for Terminalâ^'Bridging Exchange in the cis Isomer. Organometallics, 2006, 25, 2248-2252.	2.3	7
599	Picture of a chelate in exchange: the crystal structure of NaHoDOTMA, a â€~semi'-hydrated chelate. Chemical Communications, 2013, 49, 2320.	4.1	7
600	Synthesis and characterization of an MRI Gdâ€based probe designed to target the translocator protein. Magnetic Resonance in Chemistry, 2013, 51, 116-122.	1.9	7
601	The hydroboration reaction as a key for a straightforward synthesis of new MRI-NCT agents. Organic and Biomolecular Chemistry, 2015, 13, 3288-3297.	2.8	7
602	Iron oxide/PLGA nanoparticles for magnetically controlled drug release. International Journal of Applied Electromagnetics and Mechanics, 2017, 53, S53-S60.	0.6	7
603	Enzymeâ€Responsive LipoCEST Agents: Assessment of MMPâ€2 Activity by Measuring the Intraâ€liposomal Water <sup>1</sup> Hâ€NMR Shift. Angewandte Chemie, 2017, 129, 12338-12341.	2.0	7
604	Generation of multiparametric MRI maps by using Gd-labelled- RBCs reveals phenotypes and stages of murine prostate cancer. Scientific Reports, 2018, 8, 10567.	3.3	7
605	Exploring the tumour extracellular matrix by in vivo Fast Field Cycling relaxometry after the administration of a Gadoliniumâ€based MRI contrast agent. Magnetic Resonance in Chemistry, 2019, 57, 845-851.	1.9	7
606	A Simple and Fast Assay Based on Carboxyfluorescein-Loaded Liposome for Quantitative DNA Detection. ACS Omega, 2020, 5, 1764-1772.	3.5	7
607	Supramolecular adducts between macrocyclic Gd( <scp>iii</scp> ) complexes and polyaromatic systems: a route to enhance the relaxivity through the formation of hydrophobic interactions. Chemical Science, 2021, 12, 1368-1377.	7.4	7
608	Chapter 3. Chemical Exchange Saturation Transfer (CEST) Contrast Agents. New Developments in NMR, 2017, , 243-317.	0.1	7
609	What do we know about dynamic glucose-enhanced (DGE) MRI and how close is it to the clinics? Horizon 2020 GLINT consortium report. Magnetic Resonance Materials in Physics, Biology, and Medicine, 2022, 35, 87-104.	2.0	7
610	Gas-phase ultraviolet photoelectron spectra of [{Ni(Î+-C5H5)}2(µ-C2R2)](R = H or CF3) complexes. Journal of the Chemical Society Dalton Transactions, 1983, , 869-872.	1.1	6
611	Deuterium isotope effects on oxygen-17 chemical shifts. Magnetic Resonance in Chemistry, 1986, 24, 919-920.	1.9	6
612	Solution structures and dynamics of [HOs3(CO)10(σ,π vinyl)] complexes. Inorganica Chimica Acta, 1986, 111, 95-98.	2.4	6

#	Article	IF	CITATIONS
613	Organomental clusters as models for corrosion inhibitors. The reaction of Os3(CO) 10(NCCH3)2 with benzotriazole. Journal of Organometallic Chemistry, 1988, 353, 251-257.	1.8	6
614	Solid state 13C CP-MAS NMR spectra of iron (alkyne) carbonyl compounds. Journal of Organometallic Chemistry, 1989, 368, 331-338.	1.8	6
615	NMR studies of L-Dopa melanin-manganese(II) complex in water solution. Journal of Inorganic Biochemistry, 1989, 36, 1-9.	3.5	6
616	Quantitative Determination of Methemoglobin by Measuring the Solvent-Water Proton-Nuclear Magnetic Resonance Relaxation Rate. Clinical Chemistry, 1992, 38, 2401-2404.	3.2	6
617	Dipolar Oscillations in the 13 C–{ 1 H} Cross-Polarization/Magic- Angle-Spinning Spectrum of H 2 Os 3 (CO) 10. Journal of Magnetic Resonance Series A, 1995, 116, 251-254.	1.6	6
618	A versatile route to [Ru3(CO)11(alkyne)] complexes. Chemical Communications, 1997, , 267-268.	4.1	6
619	NMR and luminescence studies on the formation of ternary adducts between HSA and Ln(III)–malonate complexes (Ln=Eu, Gd, Tb). BBA - Proteins and Proteomics, 1998, 1385, 7-16.	2.1	6
620	Synthesis of new polyoxapolycarboxylic ligands for lanthanide(III) ions complexation. Tetrahedron Letters, 2004, 45, 5901-5903.	1.4	6
621	Contrastâ€enhanced MRI of murine sponge model for progressive angiogenesis assessed with gadoteridol (ProHance) and gadocoletic acid trisodium salt (B22956/1). Journal of Magnetic Resonance Imaging, 2008, 27, 872-880.	3.4	6
622	Thermodynamic analysis of hydration in human serum heme–albumin. Biochemical and Biophysical Research Communications, 2009, 385, 385-389.	2.1	6
623	Supramolecular Adducts of Negatively Charged Lanthanide(III) DOTP Chelates and Cyclodextrins Functionalized with Ammonium Groups: Mass Spectrometry and Nuclear Magnetic Resonance Studies. European Journal of Inorganic Chemistry, 2012, 2012, 2087-2098.	2.0	6
624	Polymeric Vesicles Loaded with Gadoteridol as Reversible and Concentration-Independent Magnetic Resonance Imaging Thermometers. Journal of Biomedical Nanotechnology, 2014, 10, 1620-1626.	1.1	6
625	MEMRI and tumors: a method for the evaluation of the contribution of Mn(II) ions in the extracellular compartment. NMR in Biomedicine, 2015, 28, 1104-1110.	2.8	6
626	Polyhydroxylated GdDTPA-derivatives as high relaxivity magnetic resonance imaging contrast agents. RSC Advances, 2015, 5, 74734-74743.	3.6	6
627	Asparagine in plums detected by CEST–MRI. Food Chemistry, 2015, 169, 1-4.	8.2	6
628	Probing lactate secretion in tumours with hyperpolarised NMR. NMR in Biomedicine, 2016, 29, 1079-1087.	2.8	6
629	Inner-sphere water and hydrogen bonds in lanthanide DOTAM complexes. A neutron diffraction study. Inorganica Chimica Acta, 2018, 470, 433-438.	2.4	6
630	Development and characterization of lanthanide-HPDO3A-C16-based micelles as CEST-MRI contrast agents. Dalton Transactions, 2019, 48, 5343-5351.	3.3	6

#	Article	IF	CITATIONS
631	Characterization of a Manganeseâ€Containing Nanoparticle as an MRI Contrast Agent. European Journal of Inorganic Chemistry, 2019, 2019, 1759-1766.	2.0	6
632	An efficient MRI agent targeting extracellular markers in prostate adenocarcinoma. Magnetic Resonance in Medicine, 2019, 81, 1935-1946.	3.0	6
633	Towards an Improved Design of MRI Contrast Agents: Synthesis and Relaxometric Characterisation of Gdâ€HPDO3A Analogues. Chemistry - A European Journal, 2020, 26, 6056-6063.	3.3	6
634	How the catalysis of the prototropic exchange affects the properties of lanthanide(III) complexes in their applications as MRI contrast agents. Inorganica Chimica Acta, 2022, 532, 120730.	2.4	6
635	Solution structures and dynamic behaviour of some iron chalcogen derivatives. Transition Metal Chemistry, 1979, 4, 322-325.	1.4	5
636	UV photoelectron spectra of some organometallic carbonyl osmium clusters. Journal of Organometallic Chemistry, 1982, 229, C27-C30.	1.8	5
637	Oxygen-17 relaxation times of metallocarbonyls: the use of the 17O electric quadrupole coupling as a new structural probe. Journal of the Chemical Society Chemical Communications, 1983, , 794.	2.0	5
638	Gas-phase UV photoelectron spectra of some edge-bridged decacarbonyltriosmium cluster. Inorganic Chemistry, 1983, 22, 3899-3903.	4.0	5
639	Stoichiometric hydrogenation of the heterobimetallic (α-alkynyl) complex [μ(1î—,σ, 2î—,3η3î—,H2Cî—,C î—¼ Cî [(CO)3Feî—,Co(CO)3]. Polyhedron, 1984, 3, 175-181.	—_CH3)] 2:2	5
640	Crystal structure and NMR investigation of the serine proteinase inhibitor MR889, a cyclic thiolic compound. Journal of the Chemical Society Perkin Transactions II, 1993, , 2253.	0.9	5
641	High-resolution NMR and relaxometric studies of Ln(III) complexes of relevance to MRI. Journal of Alloys and Compounds, 1995, 225, 274-278.	5.5	5
642	Addition of NH3 to the Cluster Complexes M3H(μ-H)(CO)11 (M = Ru, Os). Organometallics, 1998, 17, 5353-5357.	2.3	5
643	Intramolecular hydrogen bonding in transition metal clusters: NMR evidence for an Os–Hâ∢H–S interaction in H(ݼ-H)Os3(CO)10(HSR) (R=ethyl, cyclopentyl). Inorganica Chimica Acta, 2003, 351, 251-255.	2.4	5
644	Visualization through Magnetic Resonance Imaging of DNA Internalized Following "In Vivo― Electroporation. Molecular Imaging, 2005, 4, 153535002005041.	1.4	5
645	Carbon coated microshells containing nanosized Gd(iii) oxidic phases for multiple bio-medical applications. Chemical Communications, 2008, , 5936.	4.1	5
646	CMR2009: 11.02: Evaluating iopamidol as pHâ€responsive CEST agent at 3 and 7 T. Contrast Media and Molecular Imaging, 2009, 4, 294-295.	0.8	5
647	Lanthanidesâ€based catalysis in eukaryotes. IUBMB Life, 2018, 70, 1067-1075.	3.4	5
648	Insights into Interfacial Water Structuring at the Nafion Surface by <i>T</i> <sub>1</sub> -Weighted Magnetic Resonance Imaging. Langmuir, 2020, 36, 540-545.	3.5	5

#	Article	IF	CITATIONS
649	Multilamellar LipoCEST Agents Obtained from Osmotic Shrinkage of Paramagnetically Loaded Giant Unilamellar Vescicles (GUVs). Angewandte Chemie - International Edition, 2020, 59, 2279-2283.	13.8	5
650	Monitoring tissue implants by field-cycling 1H-MRI via the detection of changes in the 14N-quadrupolar-peak from imidazole moieties incorporated in a "smart" scaffold material. Journal of Materials Chemistry B, 2021, 9, 4863-4872.	5.8	5
651	Intracellular Water Lifetime as a Tumor Biomarker to Monitor Doxorubicin Treatment via FFC-Relaxometry in a Breast Cancer Model. Frontiers in Oncology, 2021, 11, 778823.	2.8	5
652	Nuclear magnetic resonance spectroscopy characterization and iron content determination of human mesencephalic neuromelanin. Advances in Neurology, 1996, 69, 263-70.	0.8	5
653	New tools to investigate tumor metabolism by NMR/MRI. Journal of Magnetic Resonance, 2022, 338, 107198.	2.1	5
654	The 1H And 2H NMR Spectra Of HFeCo3 (CO)12. Polyhedron, 1983, 2, 1235-1240.	2.2	4
655	μ3-S bonding mode in H2M3(CO)9S clusters of Ru and Os. An UVî—,PES and theoretical study. Inorganica Chimica Acta, 1984, 84, 95-100.	2.4	4
656	Thermal and photochemical behaviour of organotetraruthenium clusters: solution structures and dynamics of phosphine-substituted derivatives. Journal of the Chemical Society Dalton Transactions, 1987, , 349.	1.1	4
657	Solution structure and dynamic behaviour of two isomers of [Fe3(CO)9{P(OR3)}3](R = Me, Et, or Ph) derivatives. Journal of the Chemical Society Dalton Transactions, 1989, , 1277.	1.1	4
658	High-resolution NMR studies of (diphosphine)(diene) rhodium complexes in the solid state. Journal of Organometallic Chemistry, 1993, 463, 223-226.	1.8	4
659	1H MAS NMR Spectra of Transition Metal Carbonyl Hydrides. Inorganic Chemistry, 1995, 34, 3557-3559.	4.0	4
660	An NMR relaxometric indicator of the formation of OH? radicals in fenton-type reactions. Chemical Communications, 1996, , 1509.	4.1	4
661	A novel 19F-NMR method for the investigation of the antioxidant capacity of biomolecules and biofluids. Free Radical Biology and Medicine, 1999, 27, 356-363.	2.9	4
662	Facile oxidative addition/reductive elimination of HX (X=Cl, Br, I) on (μ-H)2Os3(CO)10. Journal of Organometallic Chemistry, 2000, 593-594, 135-141.	1.8	4
663	Enhanced mobility of the cluster Ru3(CO)12 in the solid state formed in situ by the reaction of CO and Ru3(CO)6(μ-CO)(μ3â^¶Î·2â^¶Î·3â^¶Î·5-C12H8) on silica. Chemical Communications, 2000, , 1425-1426.	4.1	4
664	The effect of ligand basicity on the unconventional hydrogen-bond in H(μ-H)Os3(CO)10L (L=amine) derivatives. Inorganica Chimica Acta, 2002, 334, 448-454.	2.4	4
665	Determination of ferric heme-human serum albumin by 1H NMR relaxometry. Journal of Inorganic Biochemistry, 2003, 95, 64-67.	3.5	4
666	Synthesis and characterization of a macrocyclic Schiff base GdIII complex as a relaxation agent for a faster acquisition of 2H NMR spectra of ethanol. Inorganica Chimica Acta, 2004, 357, 1374-1380.	2.4	4

#	Article	IF	CITATIONS
667	Isolation of a 177Hf Complex Formed by β-Decay of a 177Lu-Labeled Radiotherapeutic Compound and NMR Structural Elucidation of the Ligand and its Lu and Hf Complexes. Inorganic Chemistry, 2009, 48, 3114-3124.	4.0	4
668	Synthesis and testing of a pâ€H <sub>2</sub> hyperpolarized <sup>13</sup> C probe based on the pyrazolo[1,5â€ <i>a</i> ]pyrimidineacetamide DPAâ€713, an MRI vector to target the peripheral benzodiazepine receptors. Magnetic Resonance in Chemistry, 2011, 49, 795-800.	1.9	4
669	Advances in bio-imaging: A survey from WWMR 2010. Journal of Magnetic Resonance, 2011, 209, 109-115.	2.1	4
670	Evidence for the Role of Intracellular Water Lifetime as a Tumour Biomarker Obtained by Inâ€Vivo Field ycling Relaxometry. Angewandte Chemie, 2018, 130, 7590-7594.	2.0	4
671	No Lanthanidesâ€based Catalysis in Eukaryotes. IUBMB Life, 2018, 71, 398-399.	3.4	4
672	Magnetic Resonance Imaging Reveals Distinct Roles for Tissue Transglutaminase and Factor XIII in Maternal Angiogenesis During Early Mouse Pregnancy. Arteriosclerosis, Thrombosis, and Vascular Biology, 2019, 39, 1602-1613.	2.4	4
673	Manganese-enhanced MRI (MEMRI) in breast and prostate cancers: Preliminary results exploring the potential role of calcium receptors. PLoS ONE, 2020, 15, e0224414.	2.5	4
674	Relaxometric Studies of Gd-Chelate Conjugated on the Surface of Differently Shaped Gold Nanoparticles. Nanomaterials, 2020, 10, 1115.	4.1	4
675	[Gd(AAZTA)] â^' Derivatives with n â€Alkyl Acid Side Chains Show Improved Properties for Their Application as MRI Contrast Agents**. Chemistry - A European Journal, 2021, 27, 1849-1859.	3.3	4
676	An albumin-binding Gd-HPDO3A contrast agent for improved intravascular retention. Inorganic Chemistry Frontiers, 2021, 8, 4014-4025.	6.0	4
677	The interaction between iodinated Xâ€ray contrast agents and macrocyclic <scp>GBCAs</scp> provides a signal enhancement in <scp>T<sub>1</sub>â€weighted MR</scp> images: Insights into the renal excretion pathways of <scp>Gdâ€HPDO3A</scp> and iodixanol in healthy mice. Magnetic Resonance in Medicine, 2022, 88, 357-364.	3.0	4
678	An NMR relaxation study of aqueous solutions of Gd(III) chelates. Journal of Magnetic Resonance, 1991, 92, 572-580.	0.5	3
679	Solid-state 31P NMR vs. solution study of bis(tertiary phosphines). Solid State Nuclear Magnetic Resonance, 1993, 2, 245-251.	2.3	3
680	1H and 13C NMR study of cyclopentadienyl metal carbonyls in the solid state. Spectrochimica Acta Part A: Molecular Spectroscopy, 1993, 49, 1307-1314.	0.1	3
681	1H-NMR relaxometric study of pancreatic serine (pro)enzyme inhibition by a Gd(III) chelate bearing boronic functionalities. IUBMB Life, 1996, 39, 741-746.	3.4	3
682	NorDATA: An original ligand based on the norbornane skeleton. Synthesis and thermodynamic characterization of metal complexes. Polyhedron, 2008, 27, 3683-3687.	2.2	3
683	Glucan Particles Loaded with Fluorinated Emulsions: A Sensitivity Improvement for the Visualization of Phagocytic Cells by <sup>19</sup> F-MRI. Current Molecular Imaging, 2015, 4, 29-34.	0.7	3
684	Diolein Based Nanostructures as Targeted Theranostics. Journal of Biomedical Nanotechnology, 2016, 12, 1076-1088.	1.1	3

#	Article	IF	CITATIONS
685	Synthesis and Relaxometric Characterization of New Poly[ <i>N</i> , <i>N</i> â€bis(3â€aminopropyl)glycine] (PAPGly) Dendrons Gdâ€Based Contrast Agents and Their <i>in Vivo</i> Study by Using the Dynamic Contrastâ€Enhanced MRI Technique at Low Field (1 T). Chemistry and Biodiversity, 2019, 16, e1900322.	2.1	3
686	Singulettâ€Kontrastâ€Magnetresonanztomographie: Freisetzung der Hyperpolarisation durch den Metabolismus**. Angewandte Chemie, 2021, 133, 6866-6873.	2.0	3
687	Low-Field NMR Relaxometry for Intraoperative Tumour Margin Assessment in Breast-Conserving Surgery. Cancers, 2021, 13, 4141.	3.7	3
688	H-Bonding and intramolecular catalysis of proton exchange affect the CEST properties of Eu <sup>III</sup> complexes with HP-DO3A-like ligands. Chemical Communications, 2021, 57, 3287-3290.	4.1	3
689	XNAT-PIC: Extending XNAT to Preclinical Imaging Centers. Journal of Digital Imaging, 2022, 35, 860-875.	2.9	3
690	Highly Sensitive "Off/On―EPR Probes to Monitor Enzymatic Activity. Chemistry - A European Journal, 2022, 28, .	3.3	3
691	Multinuclear magnetic resonance studies. I. Tetramethyldiphosphine-13C. Journal of Magnetic Resonance, 1974, 13, 236-238.	0.5	2
692	Photochemistry of hydrido ruthenium clusters. Inorganica Chimica Acta, 1984, 81, L11-L13.	2.4	2
693	Synthesis and VT-NMR studies of cationic hydride platinum clusters. Journal of Cluster Science, 1994, 5, 523-533.	3.3	2
694	Synthesis and characterization of a novel macrocyclic ligand containing nine donor atoms. Recueil Des Travaux Chimiques Des Pays-Bas, 2010, 115, 94-98.	0.0	2
695	MRI Contrast Agents: State of the Art and New Trends. , 2011, , 223-251.		2
696	The Role of the Amino Protecting Group during Parahydrogenation of Protected Dehydroamino Acids. Journal of Physical Chemistry A, 2015, 119, 11271-11279.	2.5	2
697	MRI. , 2017, , 227-324.		2
698	1H-NMR and MALDI-TOF MS as metabolomic quality control tests to classify platelet derived medium additives for GMP compliant cell expansion procedures. PLoS ONE, 2018, 13, e0203048.	2.5	2
699	Chemistry of Molecular Imaging: An Overview. , 2021, , 423-443.		2
700	Analysis of the Gadolinium retention in the Experimental Autoimmune Encephalomyelitis (EAE) murine model of Multiple Sclerosis. Journal of Trace Elements in Medicine and Biology, 2021, 68, 126831.	3.0	2
701	Multilamellar LipoCEST Agents Obtained from Osmotic Shrinkage of Paramagnetically Loaded Giant Unilamellar Vescicles (GUVs). Angewandte Chemie, 2020, 132, 2299-2303.	2.0	2
702	NONACARBONYL-μ-HYDRIDO (μ3-η3-1,3 DIMETHYL 3 ALLENYL) Triangulo-TRIRUTHENIUM (3 Ru-Ru) and NONACARBONYL-μ-HYDRIDO (μ3-η3-1,3 DIMETHYL ALLYL)Triangulo TRIRUTHENIUM (3 Ru-Ru). , 1988, , 253-	255.	2

#	Article	IF	CITATIONS
703	NMR Relaxation Studies of Polynuclear Hydrides Derivatives. , 2001, , 351-374.		2
704	Imaging of Dysfunctional Elastogenesis in Atherosclerosis Using an Improved Gadolinium-Based Tetrameric MRI Probe Targeted to Tropoelastin. Journal of Medicinal Chemistry, 2021, 64, 15250-15261.	6.4	2
705	The influence of strong acidic proton donors on the reactivity of H2Ir(CO)Cl(PPh3)2 with D2. Journal of Molecular Catalysis A, 2003, 204-205, 371-379.	4.8	1
706	Paramagnetic Metal Complexes As Contrast Agents for Magnetic Resonance Imaging. , 2005, , 541-560.		1
707	A New, Easy Access to the 6-Aminoperhydro-1,4-diazepine Scaffold under Ultrasound and Microwave Irradiation. Synthesis, 2008, 2008, 1879-1882.	2.3	1
708	Imaging probes—Introduction. Bioorganic and Medicinal Chemistry, 2011, 19, 1022.	3.0	1
709	Lipid-Based Nanoparticles in Cardiovascular Molecular Imaging. Current Cardiovascular Imaging Reports, 2013, 6, 69-75.	0.6	1
710	Contrast Media. , 2016, , 59-70.		1
711	A relaxometric method for the assessment of intestinal permeability based on the oral administration of gadoliniumâ€based MRI contrast agents. NMR in Biomedicine, 2016, 29, 475-482.	2.8	1
712	A Novel Class of 1 Hâ€MRI Contrast Agents Based on the Relaxation Enhancement Induced on Water Protons by 14 Nâ€Containing Imidazole Moieties. Angewandte Chemie, 2021, 133, 4254-4260.	2.0	1
713	LipHosomes: Reporters for Ligand/Antiâ€Ligand Assays Based On pH Readout. Analysis & Sensing, 2021, 1, 48-53.	2.0	1
714	Contrast Agents for Magnetic Resonance Imaging: A Novel Route to Enhanced Relaxivities Based on the Interaction of a GdIII Chelate with Polycyclodextrins. Chemistry - A European Journal, 1999, 5, 1253-1260.	3.3	1
715	Chapter 14 Saturating CompartmentalizedWater Protons: Liposome- and Cell-Based CEST Agents. , 2017, , 311-344.		1
716	Effects of Cations on HPTS Fluorescence and Quantification of Free Gadolinium Ions in Solution; Assessment of Intracellular Release of Gd3+ from Gd-Based MRI Contrast Agents. Molecules, 2022, 27, 2490.	3.8	1
717	Studies of the hydrophobic interaction between a pyrene-containing dye and a tetra-aza macrocyclic gadolinium complex. Inorganic Chemistry Frontiers, 2022, 9, 3494-3504.	6.0	1
718	Dynamic properties of the trinuclear carbonyl cluster FeCo2(CO)9S and its Derivatives. Inorganica Chimica Acta, 1978, 31, 291.	2.4	0
719	Mixed iron and cobalt acetylenic carbonyl derivatives. Inorganica Chimica Acta, 1980, 40, X118.	2.4	0

#	Article	IF	CITATIONS
721	Chemical Shift and Relaxation Reagents in NMR*. , 1999, , 253-261.		0
722	CMR 2005: 13.07: Novel applications in the field of MRI CEST agents. Contrast Media and Molecular Imaging, 2006, 1, 89-89.	0.8	0
723	New Radiotracers, Reporter Probes and Contrast Agents. , 0, , 191-221.		0
724	CMR 2007: 7.05: Gdâ€loaded nanosized systems for MR visualization of tumor cells. Contrast Media and Molecular Imaging, 2007, 2, 290-291.	0.8	0
725	Response to â€~Advisory about gadolinium calls for caution in the treatment of uremic patients with lanthanum carbonate'. Kidney International, 2008, 74, 536-537.	5.2	0
726	CMR2009: 5.09: B25716/1: a novel Gdâ€AAZTAâ€based MRI agent with albumin binding properties. Contrast Media and Molecular Imaging, 2009, 4, 276-277.	0.8	0
727	Society Spotlight: European Commission-supported development of targeted nanomedicines: did MediTrans make a difference?. Therapeutic Delivery, 2011, 2, 861-864.	2.2	0
728	Dose estimation in B16 tumour bearing mice for future irradiation in the thermal column of the TRIGA reactor after B/Gd/LDL adduct infusion. Applied Radiation and Isotopes, 2011, 69, 1842-1845.	1.5	0
729	Nature-inspired particles as carriers for multimodal molecular imaging applications. , 2012, , .		0
730	Preliminary in vitro and in vivo evaluation of liposomal nanoparticles for passive and active tumour targeting by scintigraphic and MRI imaging. EJNMMI Physics, 2014, 1, A82.	2.7	0
731	Società Chimica Italiana Prizes 2014. Angewandte Chemie - International Edition, 2015, 54, 1070-1071.	13.8	0
732	Chemical Shift and Relaxation Reagents in NMR â~†. , 2017, , 195-202.		0
733	An Improved Biocompatible Probe for Photoacoustic Tumor Imaging Based on the Conjugation of Melanin to Bovine Serum Albumin. Applied Sciences (Switzerland), 2020, 10, 8313.	2.5	0
734	MR Contrast Agents. , 2011, , 165-193.		0
735	NONACARBONYL-μ-DIHYDRIDO (μ3-η2-2-PENTYNE)Triangulo-TRIRUTHENIUM (3 Ru-Ru). , 1988, , 258-259.		0
736	NONACARBONYL-μ-HYDRIDO (μ3-η2-t-BUTYLETYNYL)Triangulo-TRIRUTHENIUM (3 Ru-Ru). , 1988, , 256-257.		0